Conformational selectivity and high-affinity binding in the complexation of *N*-phenyl amides in water by a phenyl extended calix[4]pyrrole

L. Escobar,[a,b] A. Díaz-Moscoso,[a] and P. Ballester*[a,c]

[a] Institute of Chemical Research of Catalonia (ICIQ), The Barcelona Institute of Science and Technology (BIST), Av. Països Catalans, 16, 43007-Tarragona, Spain. E-mail: pballester@iciq.es

[b] Universitat Rovira i Virgili, Departament de Química Analítica i Química Orgànica, c/Marcel·lí Domingo, 1, 43007-Tarragona, Spain

[c] ICREA, Pg. Lluís Companys, 23, 08018-Barcelona, Spain

Supporting Information - *Table of Contents*

1. General experimental information

Reagents and solvents were purchased from commercial sources and used without further purification unless otherwise stated. When required, dried and deoxygenated solvents supplied by Sigma-Aldrich Solvent Purification System were employed. Pyrrole was freshly distilled under vacuum prior to use. Methyltributylammonium chloride (MTBACl) was purchased as aqueous solution, dried under vacuum and employed as a solid. Thin-layer chromatography (TLC) was performed on silica gel 60 F254 (Merck). Silica gel 60 Å for chromatography (SDS) was employed in flash column chromatography. ^{1}H NMR, ^{13}C NMR, COSY, NOESY, HSQC and HMBC spectra were recorded using a Bruker 400 UltrashieldTM (400 MHz), Bruker Avance 500 UltrashieldTM (500 MHz) or Bruker Avance 500 with cryoprobe (500 MHz) spectrometers. Usual spectral abbreviations are employed with the addition of "br" for broad and "app" for apparent. Residual solvent peaks were employed for calibration of NMR spectra.[1] Mass spectrometry experiments were performed on a LCT Premier, Waters-Micromass ESI. FT-IR measurements were carried out on a Bruker Optics ATR FT-IR Alpha-p spectrometer equipped with a DTGS detector, KBr beam splitter at 4 cm^{-1} resolution.

α,α,α,α-Tetra-phenyl tetra-(3-chloro-propyl) calix[4]pyrrole **2** was prepared following a procedure previously reported in literature.[2]

1.1. Molecular modelling studies

The energy-minimized structures (PM3 using water COSMO model) of the inclusion complexes were obtained using SCIGRESS Version FJ 2.6 (EU 3.1.9). The theoretical chemicals shifts for the proton signals of free and bound *N*-phenyl amides were computed from the energy-minimized structures at the DFT level of theory (DFT/BP86-D3/def-SV(P)) using TURBOMOLE 6.5.[3,4] TMS has been calculated with the same conditions and employed as reference. Alkyl chains and pyridinium groups were pruned to methyl groups to easy the calculations.

1.2. ^{1}H NMR titration experiments

^{1}H NMR titrations were carried out by adding aliquots of a D_2O solution of the guest into a solution of the host in the same solvent or viceversa (see the corresponding figures for details). The aliquots were added to the NMR tube (initial volume = 0.5 mL) with a glass microsyringe and NMR spectra were directly recorded after the additions. The concentration of the host or the guest (depending on the experiment) was maintained constant throughout the titration.

1.3. Determination of the binding constants from the ^{1}H NMR titration data

The ^{1}H NMR titration data obtained from the addition of incremental amounts of the guest to a solution of the host was fit to a theoretical 1:1 binding model using HypNMR 2008 Version 4.0.66. The chemical shifts for the proton signals of the free receptor (δ_{free}) were fixed. The binding constant (K_a) and the chemical shifts for the proton signals of the bound host (δ_{bound}) were refined as variables. The HypNMR software returned the values for the variable parameters (K_a and δ_{bound}).

For non-symmetrical amide derivatives, the binding constants returned from the fit using HypNMR software using a 1:1 binding model are apparent values (K_{app}). The equilibrium between rotamers and the exclusive binding of the *cis*-rotamer cannot be implemented in the binding model of the software.

In order to simulate speciation profiles of titrations taking into account the equilibrium between the two non-symmetrical amide rotamers and the exclusive binding of the *cis*-rotamer by the receptor we used the Specfit Software Version 3.0.40, in particular the Differential Kinetics Module. We introduced the theoretical kinetic model shown below that takes in consideration the existence of four rate constants that are pairwise related by two reversible equilibrium binding constants:

1) *trans* $\rightarrow$ *cis*; k_1
2) *cis* $\rightarrow$ *trans*; k_2
3) *cis* + **1** $\rightarrow$ *cis*$\subset$**1**; k_3
4) *cis*$\subset$**1** $\rightarrow$ *cis* + **1**; k_4

$K_{trans/cis} = k_1/k_2$ *and* $K_{cis\subset\mathbf{1}} = k_3/k_4$

k_1 and k_2 are the rate constant values for the isomerization process between the *trans* and *cis* non-symmetrical amides. Assuming a typical energy barrier of 20 kcal·mol^{-1} for the *trans* to *cis* interconversion this translates into a $k_1 = 0.013$ s^{-1}. The value of k_2 is calculated based on the known relationship of rate constants and equilibrium constant, $K_{trans/cis} = k_1/k_2$. For example, if $K_{trans/cis}$ determined experimentally is 99, then $k_2 = 0.013/99 = 0.00013$ s^{-1}. With respect to the kinetics of the binding process, we assume a dissociation rate k_4 in the order of 3 s^{-1}. For a $K_{cis\subset\mathbf{1}} = 10^4$ M^{-1} it will translate into $k_3 = 10^4$ M^{-1} × 3 s^{-1} = 3 × 10^4 M^{-1} s^{-1}. We also need to provide the software with initial concentrations of the amide and the receptor. We used an equilibration time of 10 s for the kinetic system to reach equilibrium and return the concentration of all the species at equilibrium. We computed a speciation simulation for each point of the titration and for a given value of $K_{cis\subset\mathbf{1}}$ (concentration of **1** is constant for all simulated speciation but the amide concentration increases in the case of a direct titration).

The concentrations of free (H_{free}) and bound host (H_{bound}) determined for the speciation at each point of the titration were used to calculate the chemical shift values (δ_c) using the following equation:

5) δ_c (ppm) = [x(H_{free}) x δ_{free}] + [x(H_{bound}) x δ_{bound}]

where x(H_{free}) = $[H]_{free}/[H]$ and x(H_{bound}) = $[H_{bound}]/[H]$; x(H_{free}) and x(H_{bound}) are the molar fractions of free host (H_{free}) and the complex (H_{bound}), respectively. The value of δ_{free} was obtained from the ^{1}H NMR spectra of the free host. The value of δ_{bound} is the chemical shift of the fully bound host determined from the fit to a simple 1:1 model.

The calculated (δ_c) chemical shifts produced a theoretical binding isotherm that was compared with the experimental binding isotherm defined by the observed (δ_{obs}) chemical shift changes of selected protons during the titrations.

We performed several simulations of the isotherm for the titrations under analysis by changing exclusively the value of $K_{cis\subset\mathbf{1}}$ until obtained a good fit of the theoretical and experimental binding isotherms based on the residual values and the visual fit of the curves.

1.4. Isothermal titration calorimetry (ITC) experiments

ITC experiments were performed in a MicroCal VP-ITC MicroCalorimeter with the VP Viewer 2000 software. Titrations were carried out by adding small aliquots (6 µL; 30 s; 180 s or 16 µL; 32 s; 180 s) of a water solution of the guest into a solution of the host in the same solvent. The concentration of guest solutions was approximately seven to ten times more concentrated than receptor solutions (see corresponding figures for details). The association constants and the thermodynamic parameters were obtained from the fit of the titration data to the “one set of sites” binding model implemented in the Microcal ITC Data Analysis module.

2. Synthetic procedures and characterization data

2.1. Tetra-phenyl tetra-(3-pyridinium-propyl) calix[4]pyrrole tetra-chloride 1

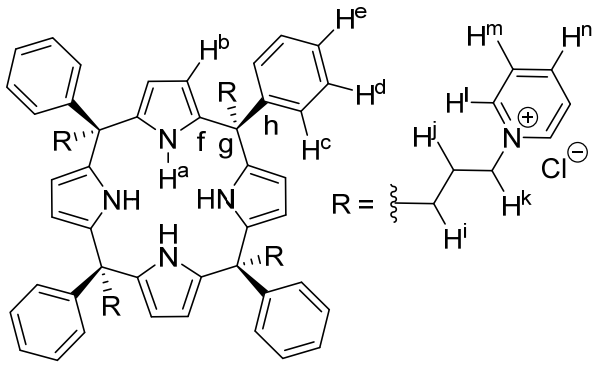

Figure S1. Line-drawing structure of tetra-pyridinium calix[4]pyrrole tetra-chloride **1**.

Tetra-chloro calix[4]pyrrole **2**[2] (80 mg, 0.086 mmol) was dissolved in pyridine (20 mL) in a 50 mL RBF and the flask was covered with foil. The mixture was stirred at 110 °C under Argon atmosphere for 24 h. The yellow precipitate was filtered off and washed with acetone (3x10 mL). Then, the solid was dissolved in deionised water and freeze-dried to yield **1** as light yellow foam (103 mg, 0.083 mmol, 96%).

^{1}H NMR (500 MHz, DMSO-d_6, 298 K): δ (ppm) = 9.08 (br s, 4H, Ha); 9.06 (dd, 8H, $^3J_{Hl\text{-}Hm}$ = 6.7 Hz, $^4J_{Hl\text{-}Hn}$ = 1.2 Hz, Hl); 8.60 (tt, 4H, $^3J_{Hn\text{-}Hm}$ = 7.8 Hz, Hn); 8.15 (dd, 8H, Hm); 7.25 (dd, 8H, $^3J_{Hd\text{-}Hc}$ = 8.3 Hz, $^3J_{Hd\text{-}He}$ = 7.3 Hz, Hd); 7.11 (tt, 4H, $^4J_{He\text{-}Hc}$ = 1.4 Hz, He); 6.80 (dd, 8H, Hc); 5.96 (d, 8H, $^4J_{Hb\text{-}Ha}$ = 2.6 Hz, Hb); 4.53 (t, 8H, $^3J_{Hk\text{-}Hj}$ = 7.1 Hz, Hk); 2.25 (br m, 8H, Hi); 1.53 (br m, 8H, Hj).

^{13}C{^{1}H} NMR (125 MHz, DMSO-d_6, 298 K): δ (ppm) = 145.6 (Cn); 145.2 (Ch); 144.6 (Cl); 136.3 (Cf); 128.2 (Cm, Cc, Cd); 127.0 (Ce); 104.8 (Cb); 60.5 (Ck); 47.3 (Cg); 36.6 (Ci); 27.2 (Cj).

HR-MS (ESI) ($C_{76}H_{76}Cl_2N_8$) $[M+2Cl]^{2+}$: Meas.: 585.2801; Calc.: 585.2780.

FT-IR (ATR) $\bar{\nu}_{max}$ (cm^{-1}): 3386; 3210; 3130; 3055; 2974; 2930; 2868; 1631; 1578; 1485; 1447; 1159; 767; 706; 684.

M.p. > 210^{o}C (decompose).

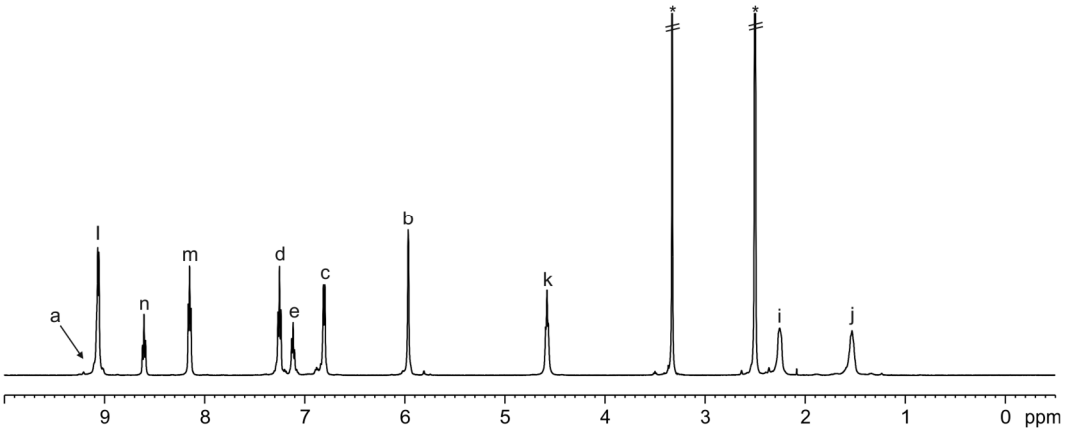

Figure S2. ^{1}H NMR (500 MHz, DMSO-d_6, 298 K) spectrum of tetra-pyridinium calix[4]pyrrole tetra-chloride **1**. See Figure S1 for proton assignments. *Solvent residual peaks.

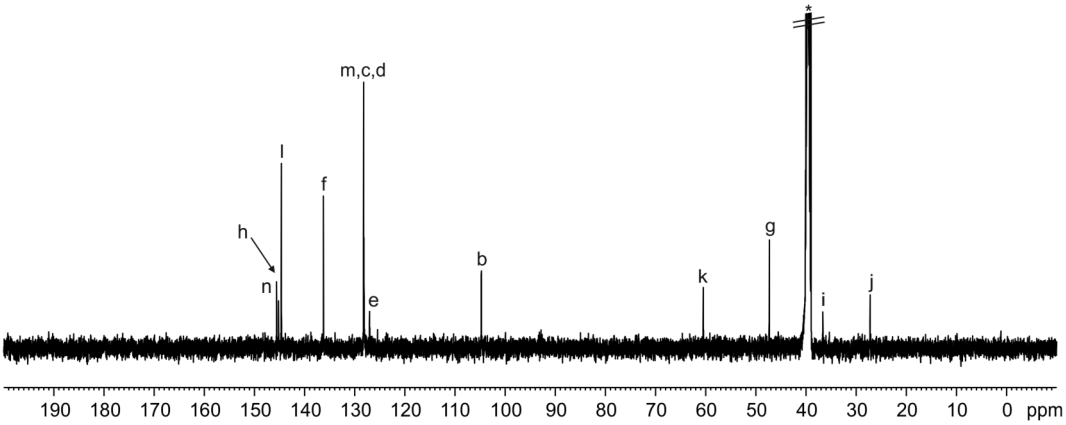

Figure S3. ^{13}C{^{1}H} NMR (125 MHz, DMSO-d_6, 298 K) spectrum of tetra-pyridinium calix[4]pyrrole tetra-chloride **1**. See Figure S1 for carbon assignments. *Solvent residual peak.

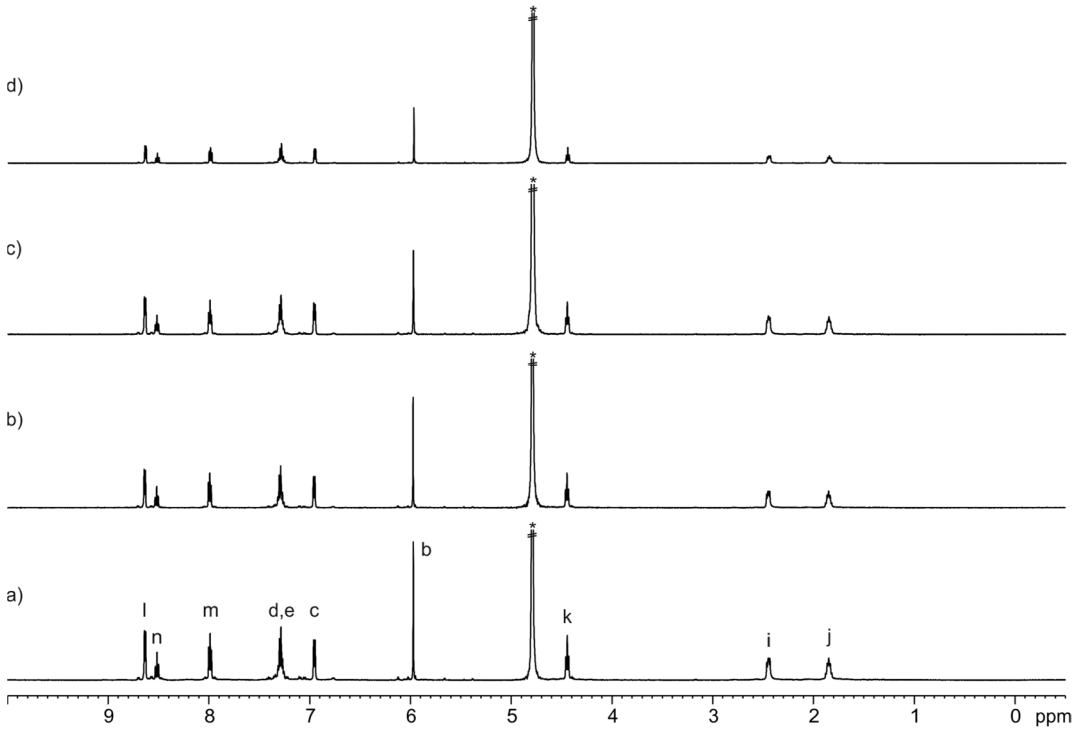

Figure S4. Dilution experiment of tetra-pyridinium calix[4]pyrrole tetra-chloride **1**. ^{1}H NMR (500 MHz with cryoprobe, D_2O, 298 K) spectra of compound **1**: a) 1 mM; b) 0.8 mM; c) 0.6 mM and d) 0.4 mM. See Figure S1 for proton assignments. *Solvent residual peaks.

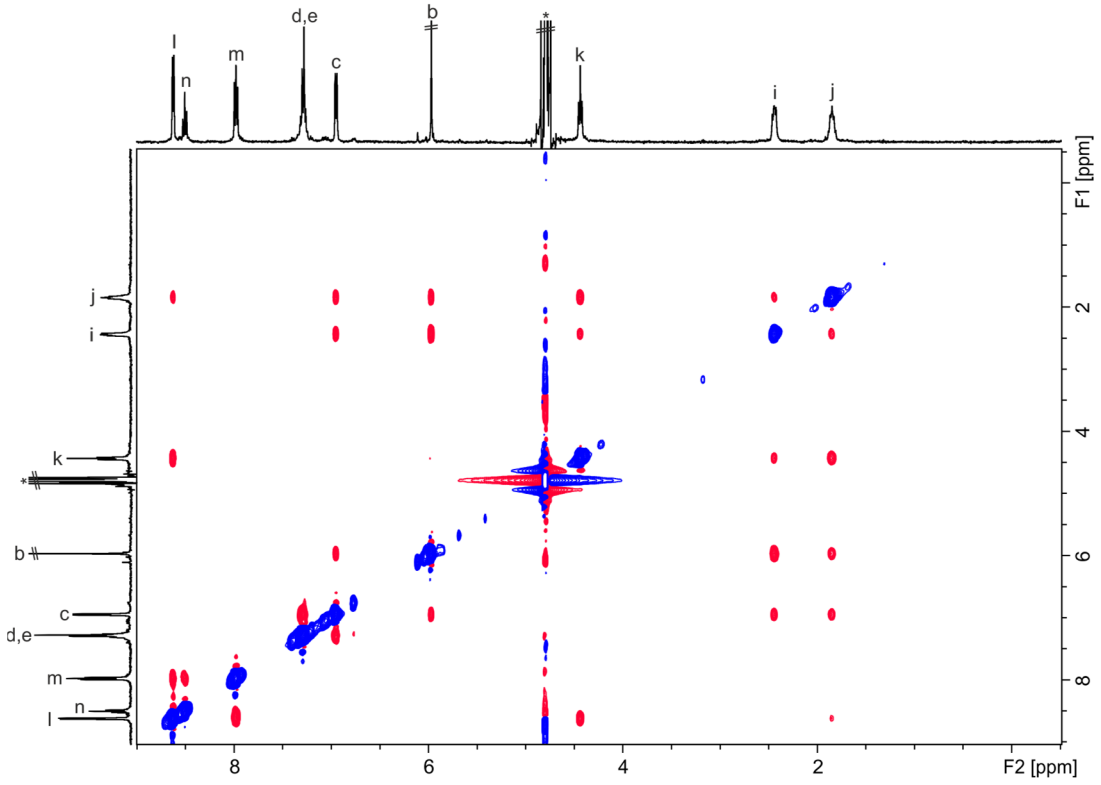

Figure S5. ^{1}H-^{1}H 2D ROESY (400 MHz, D_2O, 298 K, spin lock = 0.4 s) spectrum of tetra-pyridinium calix[4]pyrrole tetra-chloride **1**. *Solvent residual peak.

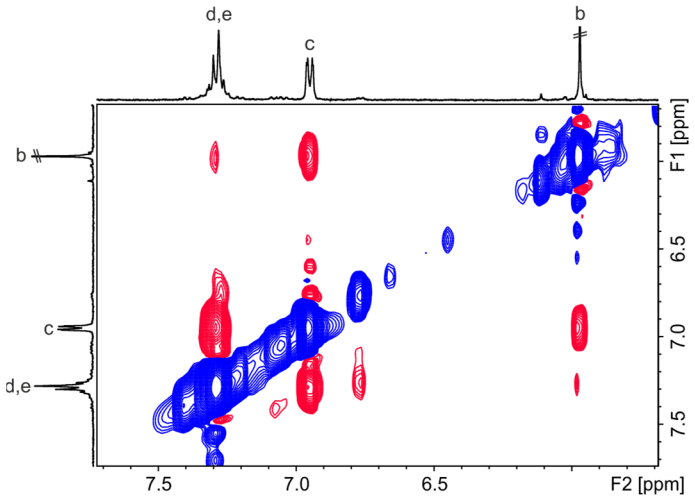

Figure S6. Selected region of the ^{1}H-^{1}H 2D ROESY (400 MHz, D_2O, 298 K, spin lock = 0.4 s) spectrum of tetra-pyridinium calix[4]pyrrole tetra-chloride **1**.

The ^{1}H-^{1}H 2D ROESY NMR spectrum of **1** showed intense cross-peaks between the H^b and H^c protons indicating close proximity. Also, cross-peaks between H^b and H^d protons of **1** were observed.

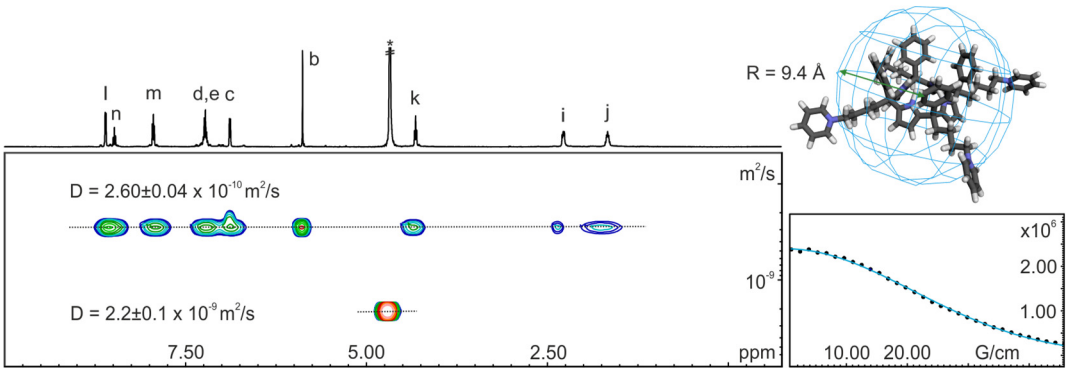

Figure S7. ^{1}H pseudo 2D DOSY NMR (500 MHz with cryoprobe, D_2O, D20 = 0.15 s, P30 = 1 ms, 298 K) experiment of tetra-pyridinium calix[4]pyrrole tetra-chloride **1** (1 mM). The data was fit to a mono-exponential function using Dynamics Center from Bruker. The hydrodynamic radius of **1** was determined using the Stokes-Einstein equation. *Solvent residual peaks.

The dilution and DOSY NMR experiments of **1** at millimolar concentrations indicated that the calix[4]pyrrole was soluble in water as discrete species.

2.2. Characterization of amides in water

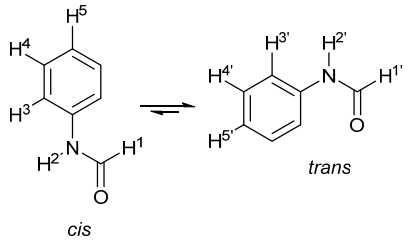

Figure S8. Conformational isomers of *N*-phenyl-formamide **3**.

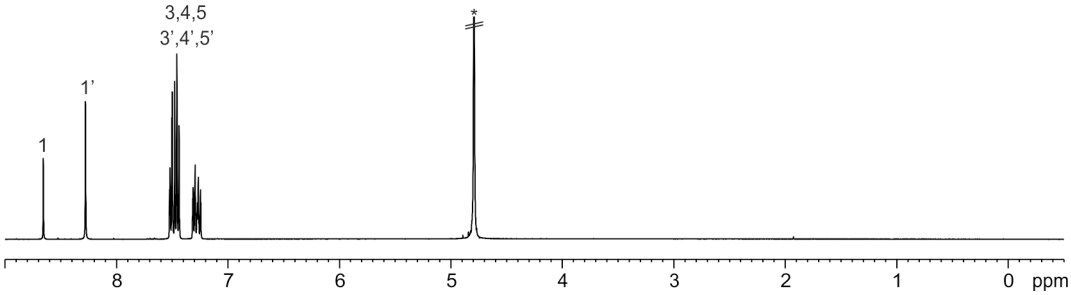

Figure S9. ^{1}H NMR (400 MHz, D_2O, 298 K) spectrum of *N*-phenyl-formamide **3**. See Figure S8 for proton assignments. *Solvent residual peaks.

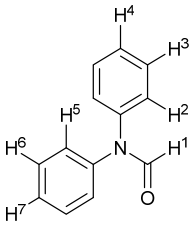

Figure S10. Structure of *N*,*N*-diphenyl-formamide **4**.

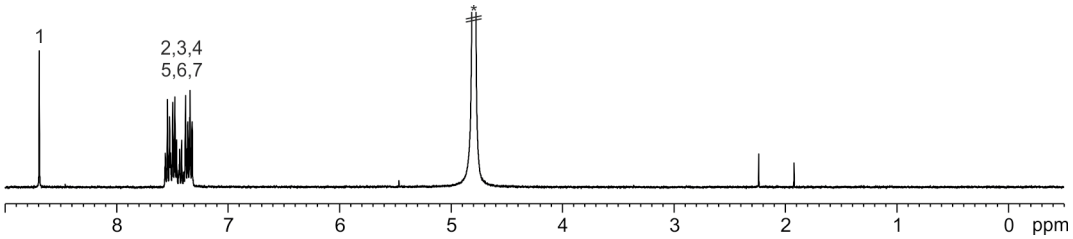

Figure S11. ^{1}H NMR (400 MHz, D_2O, 298 K) spectrum of *N*,*N*-diphenyl-formamide **4**. See Figure S10 for proton assignments. *Solvent residual peaks. The amide **4** showed a limited solubility in water.

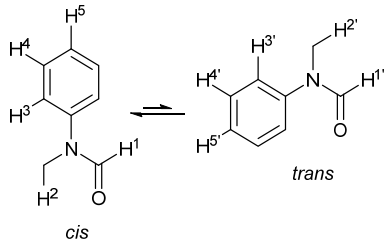

Figure S12. Conformational isomers of *N*-methyl-*N*-phenyl-formamide **5**.

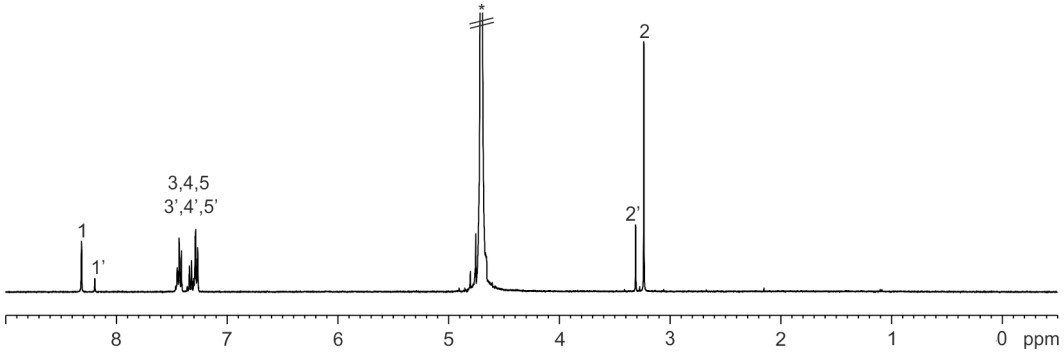

Figure S13. ^{1}H NMR (400 MHz, D_2O, 298 K) spectrum of *N*-methyl-*N*-phenyl-formamide **5**. See Figure S12 for proton assignments. *Solvent residual peaks.

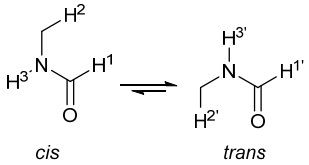

Figure S14. Conformational isomers of *N*-methyl-formamide **6**.

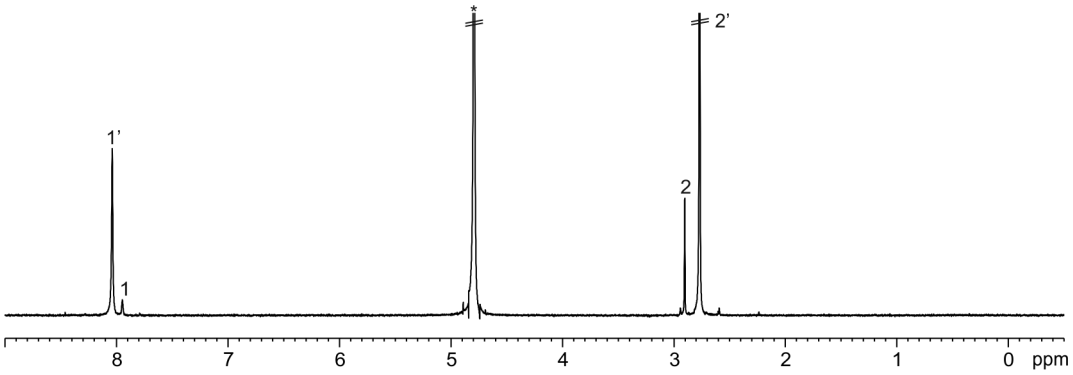

Figure S15. ^{1}H NMR (400 MHz, D_2O, 298 K) spectrum of *N*-methyl-formamide **6**. See Figure S14 for proton assignments. *Solvent residual peaks.

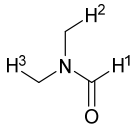

Figure S16. Structure of *N*,*N*-dimethyl-formamide **7**.

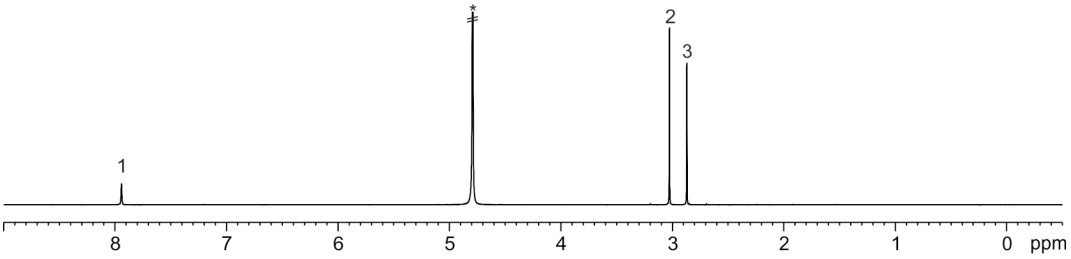

Figure S17. ^{1}H NMR (400 MHz, D_2O, 298 K) spectrum of *N*,*N*-dimethyl-formamide **7**. See Figure S16 for proton assignments. *Solvent residual peaks.

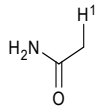

Figure S18. Structure of acetamide **8**.

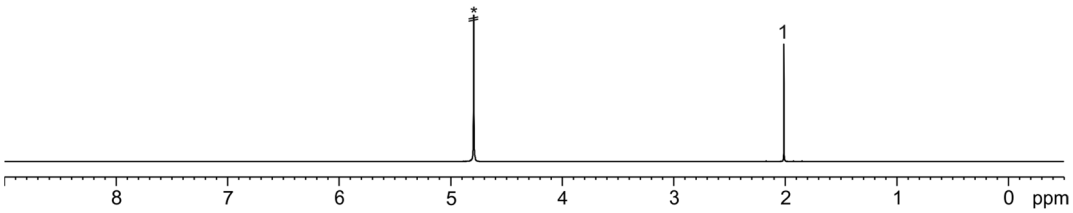

Figure S19. ^{1}H NMR (400 MHz, D_2O, 298 K) spectrum of acetamide **8**. See Figure S18 for proton assignments. *Solvent residual peaks.

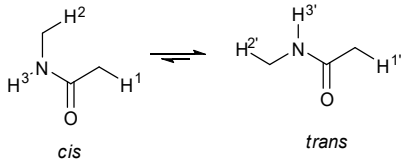

Figure S20. Conformational isomers of *N*-methyl-acetamide **9**.

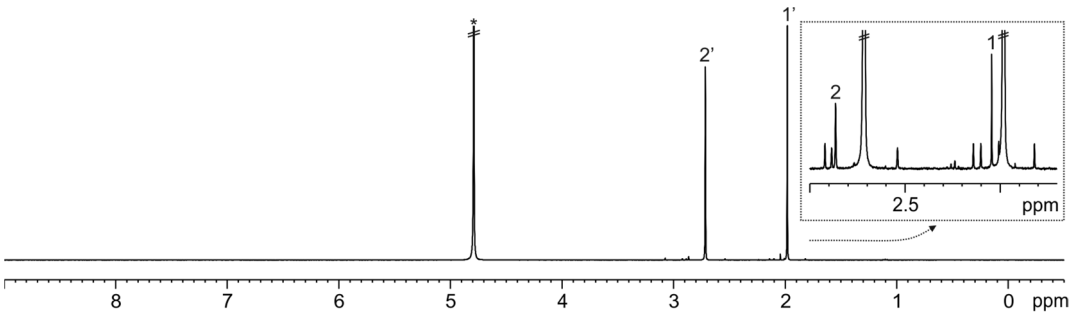

Figure S21. ^{1}H NMR (400 MHz, D_2O, 298 K) spectrum of *N*-methyl-acetamide **9**. See Figure S20 for proton assignments. *Solvent residual peaks.

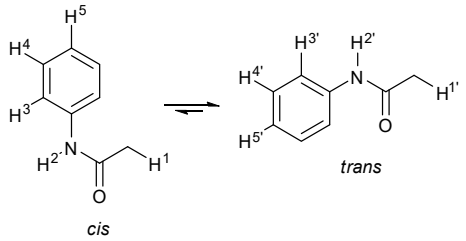

Figure S22. Conformational isomers of *N*-phenyl-acetamide **10**.

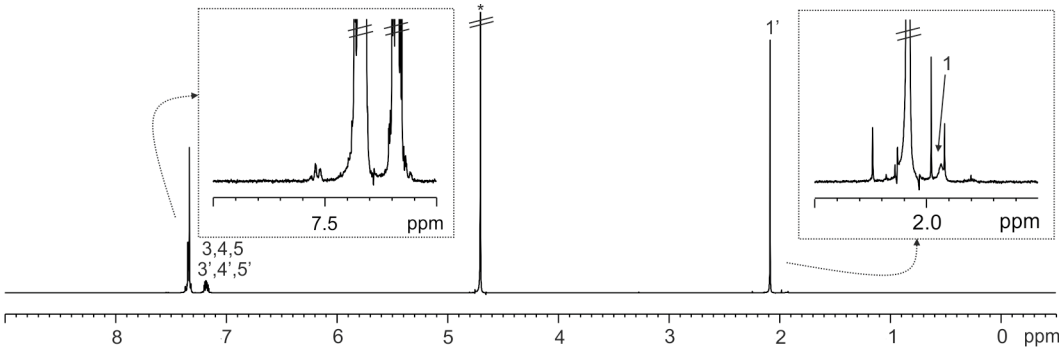

Figure S23. ^{1}H NMR (400 MHz, D_2O, 298 K) spectrum of *N*-phenyl-acetamide **10**. See Figure S22 for proton assignments. The calculated chemical shift for the CH_3 protons (H^1) of *cis*-**10** was 1.77 ppm, which was in agreement with the assignment of the proton signals in the spectrum. *Solvent residual peaks.

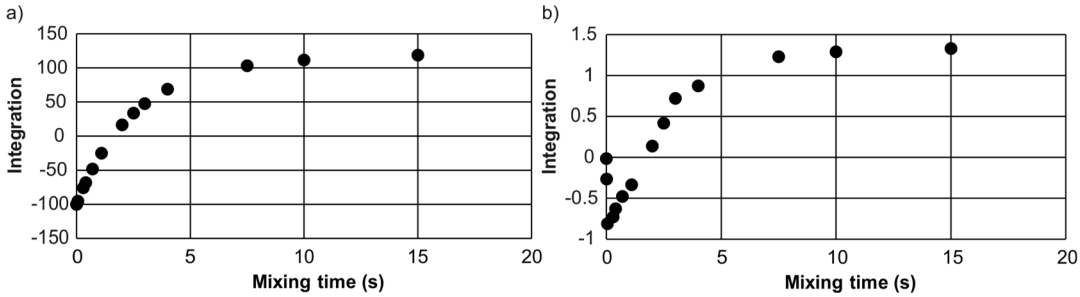

Figure S24. Integrals vs mixing time (s) for the magnetization transfer inversion recovery NMR experiment using a selective pulse sequence: a) *trans*-isomer and b) *cis*-isomer. The signal at 2.10 ppm ($H^{1'}$) corresponding to the *trans*-isomer of **10** was selectively pulsed (a). The signal at 1.90 ppm suffered a magnetization transfer due to chemical exchange (b) indicating that this proton signal (H^1) corresponded to the *cis*-isomer of **10**.

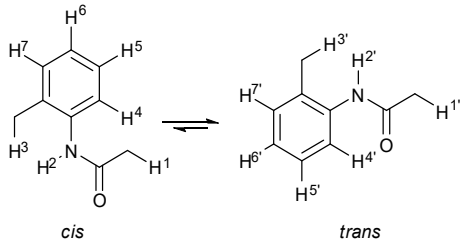

Figure S25. Conformational isomers of *O*-acetotoluidide **11**.

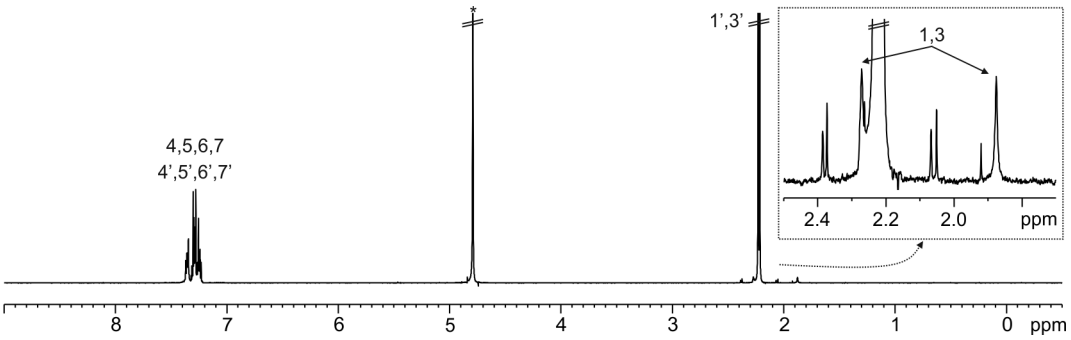

Figure S26. ^{1}H NMR (400 MHz, D_2O, 298 K) spectrum of *O*-acetotoluidide **11**. See Figure S25 for proton assignments. *Solvent residual peaks.

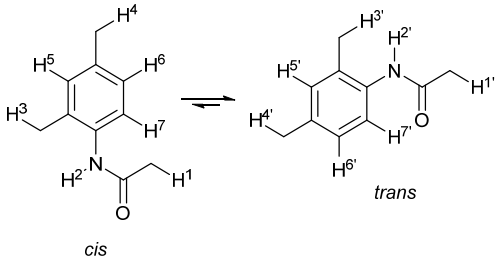

Figure S27. Conformational isomers of *N*-(2',4'-dimethylphenyl)-acetamide **12**.

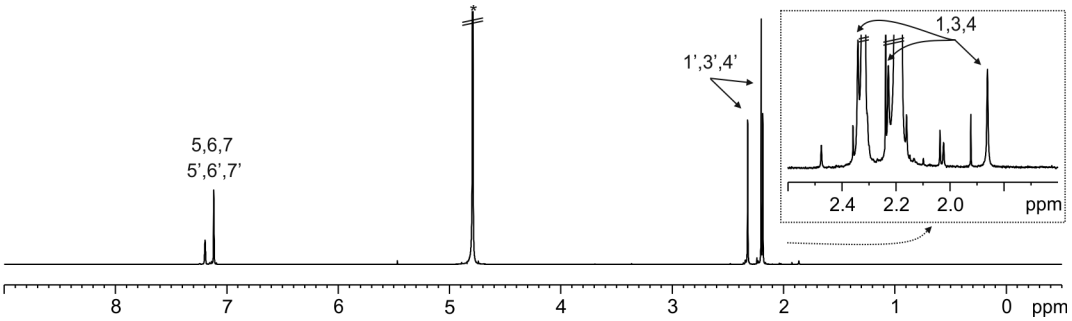

Figure S28. ^{1}H NMR (400 MHz, D_2O, 298 K) spectrum of *N*-(2',4'-dimethylphenyl)-acetamide **12**. See Figure S27 for proton assignments. *Solvent residual peaks.

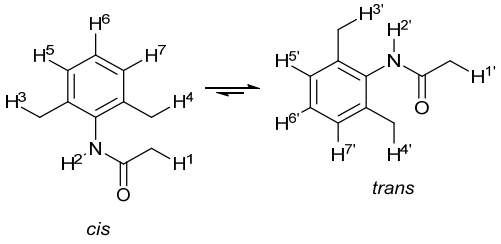

Figure S29. Conformational isomers of *N*-(2',6'-dimethylphenyl)-acetamide **13**.

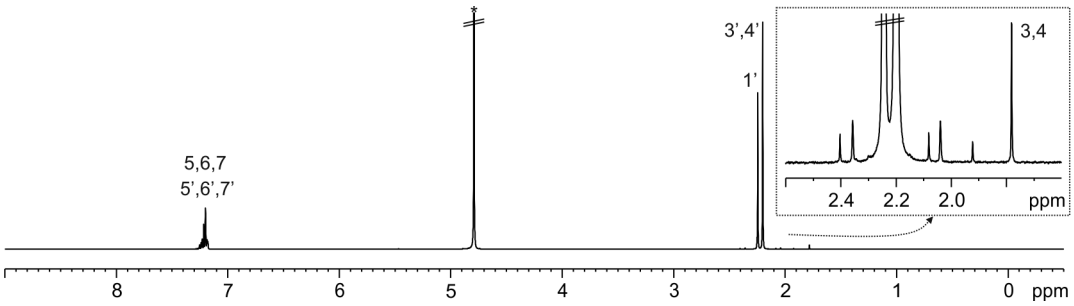

Figure S30. ^{1}H NMR (400 MHz, D_2O, 298 K) spectrum of *N*-(2',6'-dimethylphenyl)-acetamide **13**. See Figure S29 for proton assignments. *Solvent residual peaks.

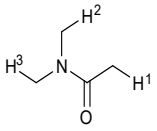

Figure S31. Structure of *N,N*-dimethyl-acetamide **14**.

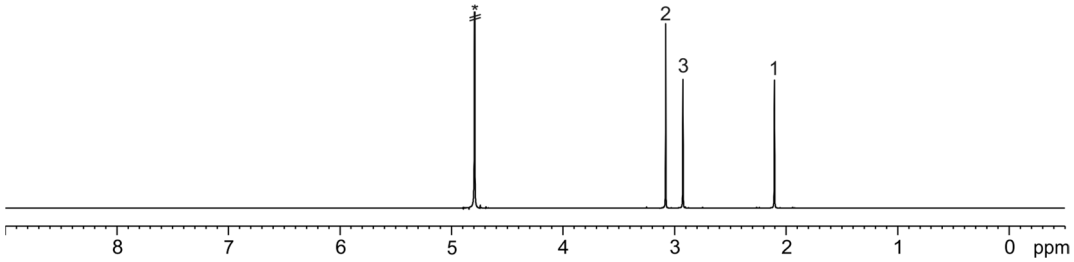

Figure S32. ^{1}H NMR (400 MHz, D_2O, 298 K) spectrum of *N*,*N*-dimethyl-acetamide **14**. See Figure S31 for proton assignments. *Solvent residual peaks.

Table S1. Molar ratio of the conformational isomers (*cis*/*trans*) of the amides in D_2O determined by integration of the ^{1}H NMR spectra and isomerization constant values (K_{iso} = [*cis*-amide]/[*trans*-amide]). The amides **4**, **7**, **8** and **14** bear identical *N*-substituents.

Amide	**3**	**4**	**5**	**6**	**7**	**8**	**9**	**10**	**11**	**12**	**13**	**14**
Molar ratio	32/68	-	82/18	8/92	-	-	1.6/98.4	1/99	2.3/97.7	2.7/97.3	2.2/97.8	-
K_{iso}	0.47	-	4.56	0.09	-	-	0.02	0.01	0.02	0.03	0.02	-

3. Molecular modeling structures

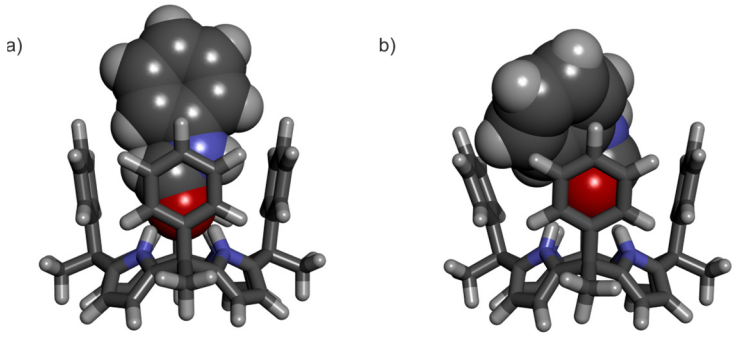

Figure S33. Energy-minimized structures (PM3, water COSMO model) of the inclusion complexes: a) *cis*-**3**⊂**1** and b) *trans*-**3**⊂**1**. The calix[4]pyrroles are depicted as stick representations and amides are shown as CPK models. For clarity, non-polar hydrogens of the calix[4]pyrroles have been omitted.

Table S2. Energies of the complexes *cis*-**3**⊂**1** and *trans*-**3**⊂**1** (PM3, water COSMO model).

Complex	E (kcal·mol^{-1})
cis-**3**⊂**1**	172.3
trans-**3**⊂**1**	179.6

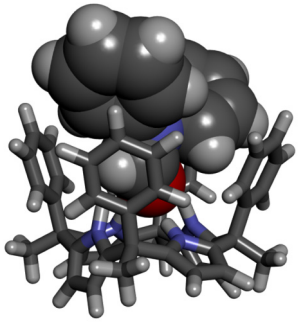

Figure S34. Energy-minimized structure (PM3, water COSMO model) of the inclusion complex **4**⊂**1**. The calix[4]pyrrole is depicted as stick representation and amide is shown as CPK model. For clarity, non-polar hydrogens of the calix[4]pyrrole has been omitted.

Table S3. Energy of the complex **4**⊂**1** (PM3, water COSMO model).

Complex	E (kcal·mol^{-1})
4⊂**1**	213.6

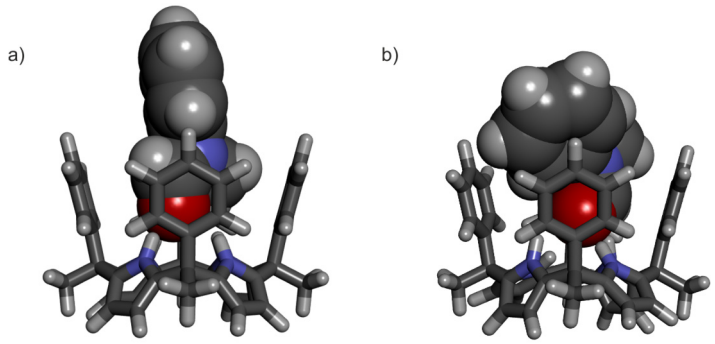

Figure S35. Energy-minimized structures (PM3, water COSMO model) of the inclusion complexes: a) *cis*-**5**⊂**1** and b) *trans*-**5**⊂**1**. The calix[4]pyrroles are depicted as stick representations and amides are shown as CPK models. For clarity, non-polar hydrogens of the calix[4]pyrroles have been omitted.

Table S4. Energies of the complexes *cis*-**5**⊂**1** and *trans*-**5**⊂**1** (PM3, water COSMO model).

Complex	**E (kcal·mol^{-1})**
cis-**5**⊂**1**	175.8
trans-**5**⊂**1**	179.9

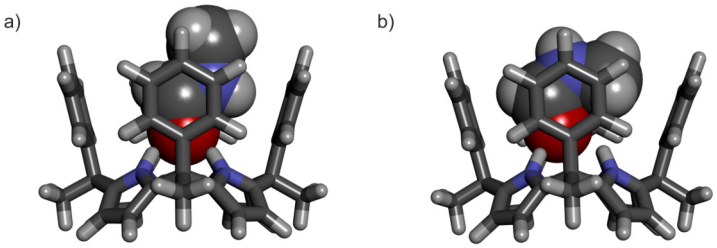

Figure S36. Energy-minimized structures (PM3, water COSMO model) of the inclusion complexes: a) *cis*-**6**⊂**1** and b) *trans*-**6**⊂**1**. The calix[4]pyrroles are depicted as stick representations and amides are shown as CPK models. For clarity, non-polar hydrogens of the calix[4]pyrroles have been omitted.

Table S5. Energies of the complexes *cis*-**6**⊂**1** and *trans*-**6**⊂**1** (PM3, water COSMO model).

Complex	**E (kcal·mol^{-1})**
E-**6**⊂**1**	147.2
Z-**6**⊂**1**	145.4

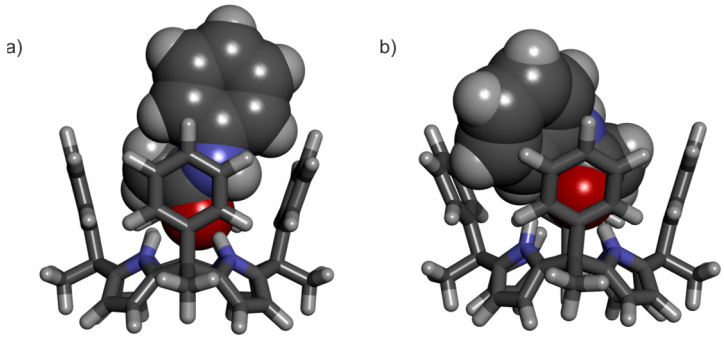

Figure S37. Energy-minimized structures (PM3, water COSMO model) of the inclusion complexes: a) *cis*-**10**⊂**1** and b) *trans*-**10**⊂**1**. The calix[4]pyrroles are depicted as stick representations and amides are shown as CPK models. For clarity, non-polar hydrogens of the calix[4]pyrroles have been omitted.

Table S6. Energies of the complexes *cis*-**10**⊂**1** and *trans*-**10**⊂**1** (PM3, water COSMO model).

Complex	**E (kcal·mol^{-1})**
cis-**10**⊂**1**	169.2
trans-**10**⊂**1**	174.3

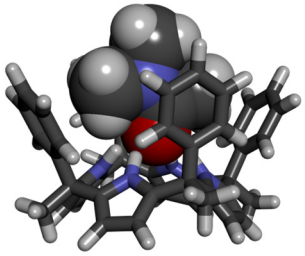

Figure S38. Energy-minimized structure (PM3, water COSMO model) of the inclusion complex **14**⊂**1**. The calix[4]pyrrole is depicted as stick representation and amide is shown as CPK model. For clarity, non-polar hydrogens of the calix[4]pyrrole has been omitted.

Table S7. Energy of the complex **14**⊂**1** (PM3, water COSMO model).

Complex	**E (kcal·mol^{-1})**
14⊂**1**	141.5

4. ^{1}H NMR binding experiments

4.1. ^{1}H NMR titration of calix[4]pyrrole 1 with *N*-phenyl-formamide 3

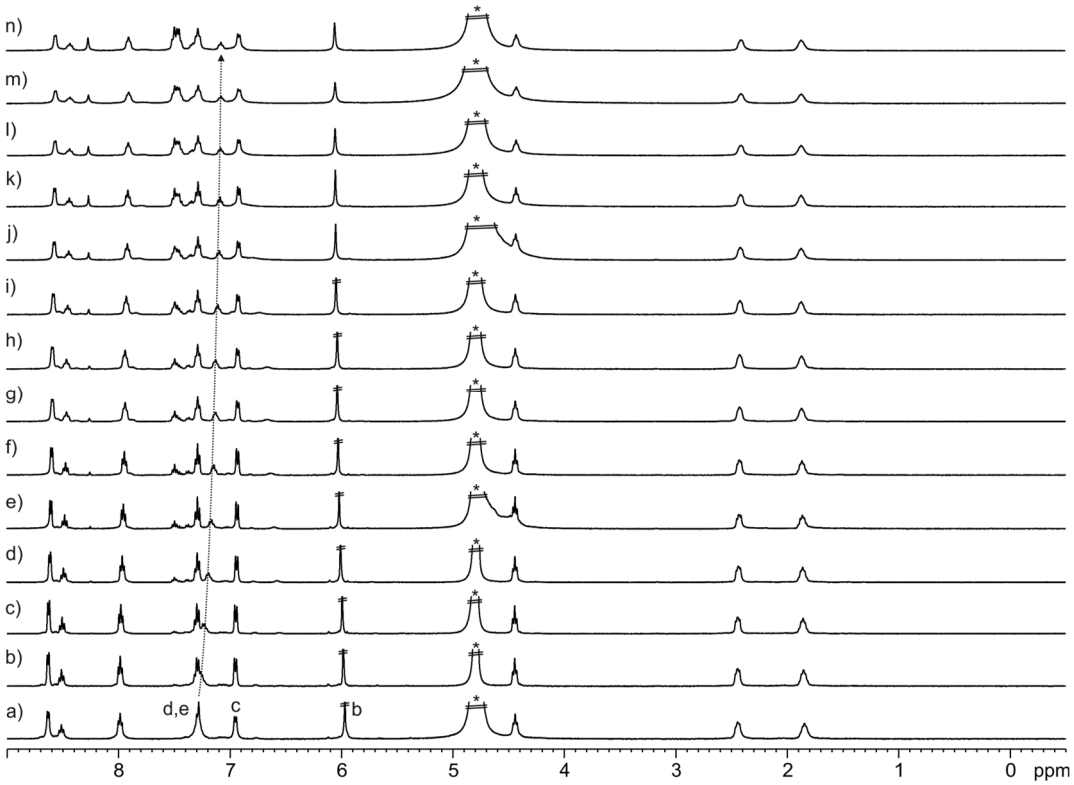

Figure S39. ^{1}H NMR (400 MHz, D_2O, 298 K) titration spectra of calix[4]pyrrole **1** (1.06 mM) with *N*-phenyl-formamide **3**: a) **1**; b) **3** + **1** (0.1:1 molar ratio); c) **3** + **1** (0.2:1 molar ratio); d) **3** + **1** (0.4:1 molar ratio); e) **3** + **1** (0.6:1 molar ratio); f) **3** + **1** (0.8:1 molar ratio); g) **3** + **1** (1:1 molar ratio); h) **3** + **1** (1.2:1 molar ratio); i) **3** + **1** (1.5:1 molar ratio); j) **3** + **1** (2:1 molar ratio); k) **3** + **1** (2.5:1 molar ratio); l) **3** + **1** (3:1 molar ratio); m) **3** + **1** (3.5:1 molar ratio) and n) **3** + **1** (4:1 molar ratio). The concentration of **1** was maintained constant through the titration. *Solvent residual peak.

The ^{1}H NMR titration spectra of the calix[4]pyrrole **1** with the formamide **3** (Figure S39) showed chemical shift changes on the proton signals of the host upon addition of incremental amounts of the guest. This result was indicative of a fast chemical exchange on the ^{1}H NMR chemical shift timescale between free and bound receptor. The proton signals of *trans*-**3** appeared sharp and well-defined but they did not display appreciable chemical shift changes respect to the free compound, indicating lack of interaction. The proton signals of *cis*-**3** appeared very broad and upfield shifted with respect to the free *cis*-amide at the initial phase of the titration experiment. This observation indicated that free and bound *cis*-**3** displayed an intermediate chemical exchange on the chemical shift timescale.

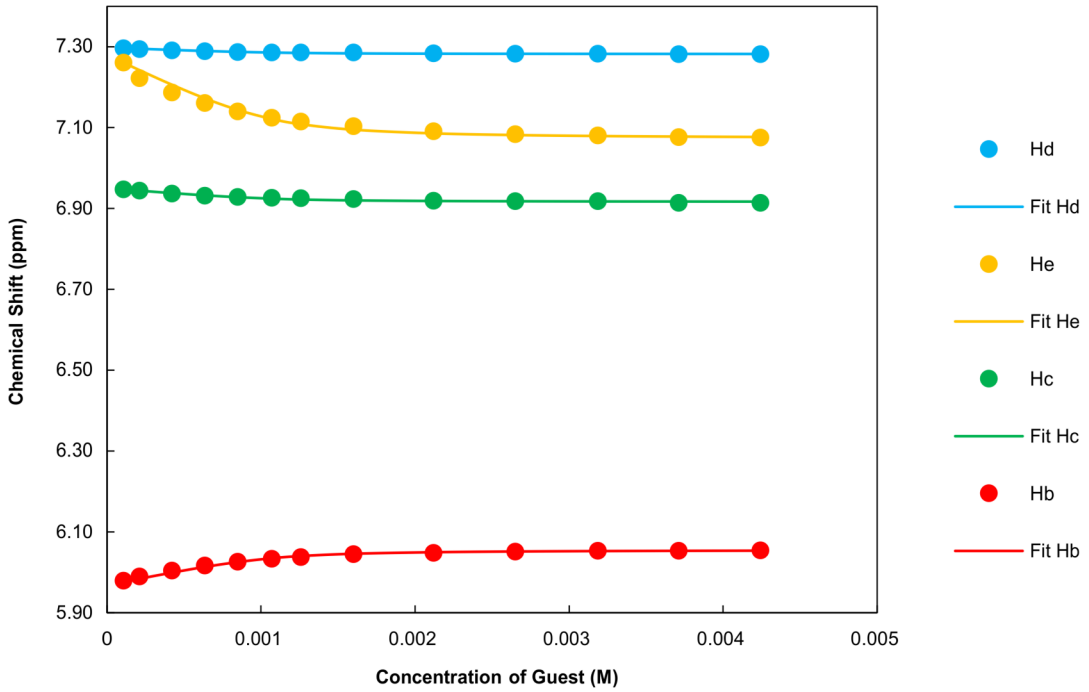

Figure S40. Fit of the ^{1}H NMR titration data (calix[4]pyrrole **1** with **3**) to a theoretical 1:1 binding model.

Table S8. Apparent binding constant returned from the fit of the ^{1}H NMR titration data (calix[4]pyrrole **1** with **3**) to a theoretical 1:1 binding model.

Amide	K_{app} (M^{-1})
3	> 10^4

Table S9. Chemical shifts for the proton signals of bound host **1** (δ_{bound}) obtained from the fit of the ^{1}H NMR titration data (calix[4]pyrrole **1** with **3**) to a theoretical 1:1 binding model and induced chemical shifts ($\Delta\delta = \delta_{bound} - \delta_{free}$).

Signal	δ_{free} (ppm)	δ_{bound} (ppm)	$\Delta\delta$ (ppm)
b	5.97	6.06	+0.09
c	6.95	6.92	-0.03
d	7.30	7.28	-0.02
e	7.28	7.07	-0.21

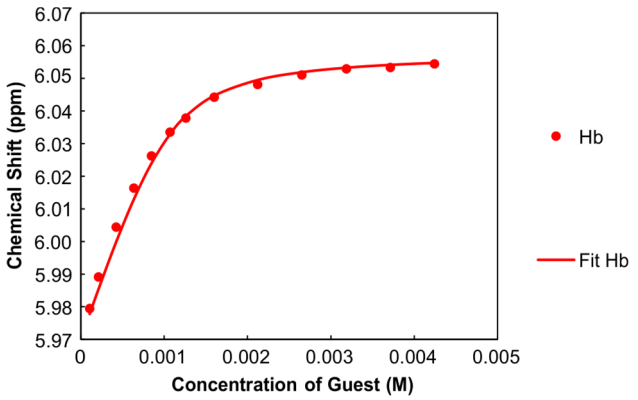

Figure S41. Fit of the ^{1}H NMR titration data (calix[4]pyrrole **1** with **3**) to the theoretical binding model considering the *cis*/*trans* equilibrium and the exclusive formation of the *cis*⊂**1** complex.

Table S10. Binding constant returned from the fit of the ^{1}H NMR titration data (calix[4]pyrrole **1** with **3**) to the theoretical binding model considering the *cis*/tr*ans* equilibrium and the exclusive formation of the *cis*⊂**1** complex.

Amide	K_a (M^{-1})
cis-**3**	> 10^4

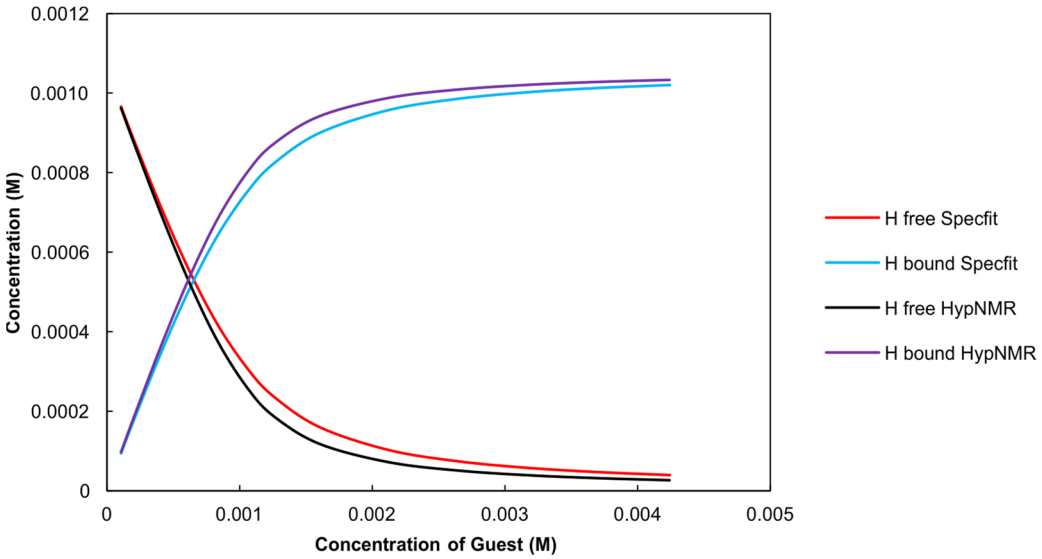

Figure S42. Calculated host (H) speciation profiles using the simple 1:1 binding model (HypNMR) and the theoretical binding model considering the *cis*/*trans* equilibrium and the exclusive formation of the *cis*⊂**1** complex (Specfit).

The speciation profiles obtained using the simple 1:1 binding model and the theoretical binding model considering the *cis*/*trans* equilibrium and the exclusive formation of the *cis*⊂**1** complex were similar. Accordingly, the two binding models returned similar estimates for the binding constant values.

4.2. ^{1}H NMR titration of *N*-phenyl-formamide 3 with calix[4]pyrrole 1

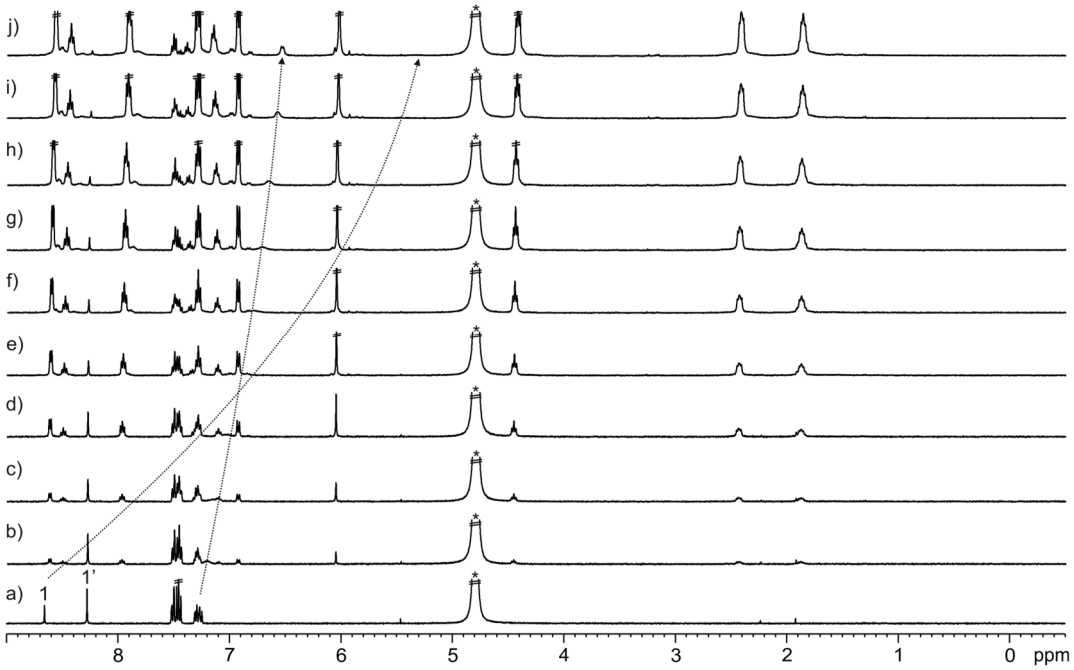

Figure S43. ^{1}H NMR (400 MHz, D_2O, 298 K) titration spectra of *N*-phenyl-formamide **3** (1.20 mM) with calix[4]pyrrole **1**: a) **3**; b) **1** + **3** (0.05:1 molar ratio); c) **1** + **3** (0.1:1 molar ratio); d) **1** + **3** (0.2:1 molar ratio); e) **1** + **3** (0.4:1 molar ratio); f) **1** + **3** (0.6:1 molar ratio); g) **1** + **3** (0.8:1 molar ratio); h) **1** + **3** (1:1 molar ratio); i) **1** + **3** (1.5:1 molar ratio) and j) **1** + **3** (2:1 molar ratio). The concentration of **3** was maintained constant through the titration. *Solvent residual peak.

The ^{1}H NMR titration spectra of the formamide **3** with calix[4]pyrrole **1** (Figure S43) showed that the addition of the receptor to a millimolar solution of **3** provoked the broadening and upfield shift of the proton signals of the *cis*-amide **3**. The proton signals of the *trans*-amide **3** (primed numbers) appeared sharp and they did not display appreciable chemical shift changes. However, the *trans*-amide proton signals decreased in intensity due to the intramolecular conformational isomerization of the amide in the bulk solution. The proton signals of the calix[4]pyrrole displayed chemical shift changes with respect to the free receptor in solution. These observations were in line with the results obtained above from the ^{1}H NMR titration experiment of calix[4]pyrrole **1** with formamide **3**.

Table S11. Experimental (δ_{obs}) and theoretical (δ_t) chemical shifts (ppm) for the proton signals of bound *cis*-**3** with the calix[4]pyrrole **1**. Experimental values were obtained from the mixture of **1** + **3** in a 2:1 molar ratio (Figure S43). The theoretical chemical shifts are in agreement with the observed counterparts.

Signal	δ_{free} (ppm)	δ_{obs} (ppm)	δ_t (ppm)	$\Delta\delta$ (ppm)
1	8.65	5.32	4.56	-3.33
2	-	-	3.88	-
3	7.28	6.53	6.10	-0.75
4	-	7.50	6.82	-
5	-	7.38	6.64	-

The experimental chemical shift of H^1 in the 2:1 mixture of **1** and **3** was assigned to a broad signal at 5.32 ppm with the help of chemical shift calculations of the *cis*-**3**⊂**1** complex.

4.3. ^{1}H NMR titration experiment of calix[4]pyrrole 1 with *N*,*N*-diphenyl-formamide 4

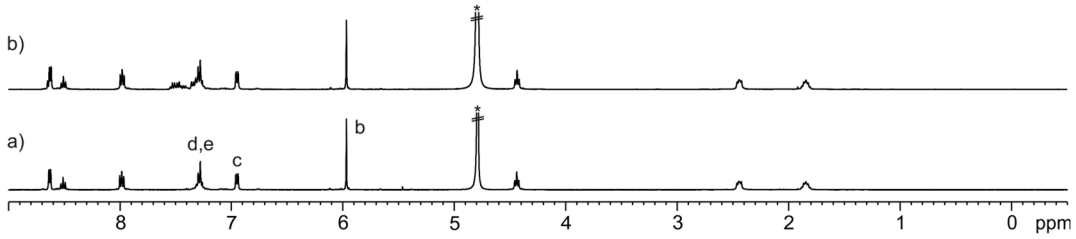

Figure S44. ^{1}H NMR (400 MHz, D_2O, 298 K) experiment of calix[4]pyrrole **1** (1.70 mM) with *N*,*N*-diphenyl-formamide **4**: a) **1**; b) **4** (excess) after sonication for 15 min.

The *N*,*N*-diphenyl-formamide **4** was added as a solid to a millimolar solution of **1** due to its low solubility (< 5 mM). The ^{1}H NMR spectra (Figure S44) showed that the addition of formamide **4** to the solution of the calix[4]pyrrole **1** did not provoke appreciable chemical shift changes on its proton signals. This result indicated that the amide **4** interacted very weakly with the receptor. Molecular modelling studies suggested that **4** was not shape and size complementary for the aromatic cavity of the receptor **1**.

4.4. ^{1}H NMR titration of calix[4]pyrrole 1 with *N*-methyl-*N*-phenyl-formamide 5

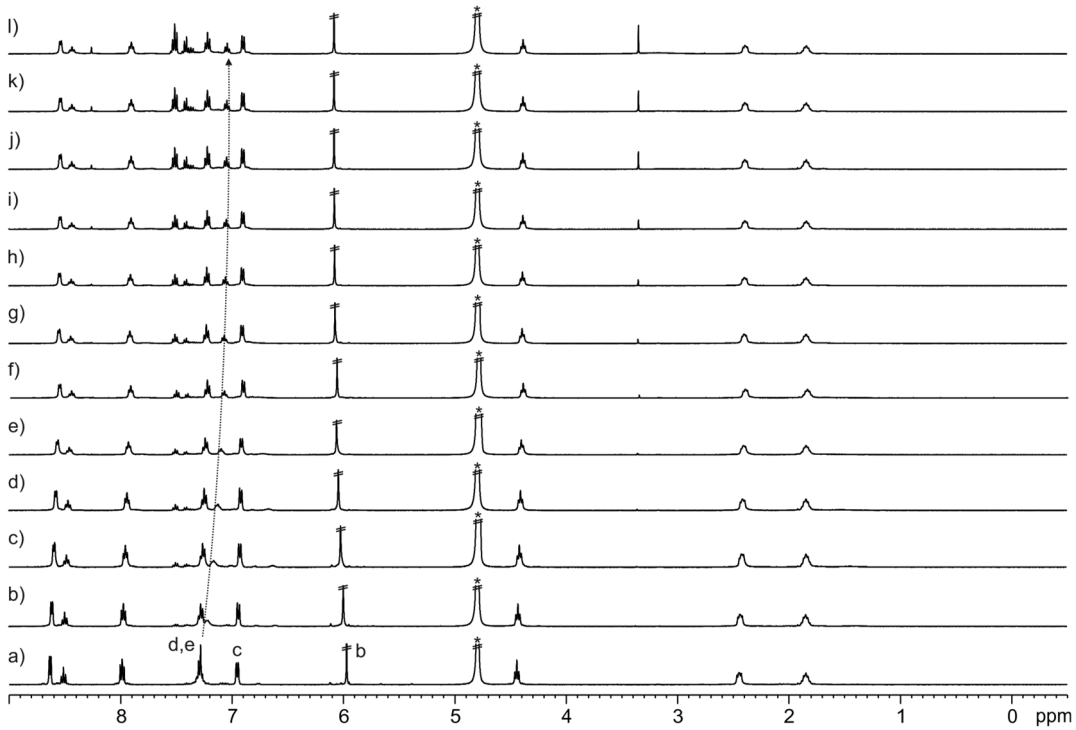

Figure S45. ^{1}H NMR (400 MHz, D_2O, 298 K) titration spectra of calix[4]pyrrole **1** (1.14 mM) with *N*-methyl-*N*-phenyl-formamide **5**: a) **1**; b) **5** + **1** (0.2:1 molar ratio); c) **5** + **1** (0.4:1 molar ratio); d) **5** + **1** (0.6:1 molar ratio); e) **5** + **1** (0.8:1 molar ratio); f) **5** + **1** (1:1 molar ratio); g) **5** + **1** (1.2:1 molar ratio); h) **5** + **1** (1.5:1 molar ratio); i) **5** + **1** (2:1 molar ratio); j) **5** + **1** (2.5:1 molar ratio); k) **5** + **1** (3:1 molar ratio) and l) **5** + **1** (4:1 molar ratio). The concentration of **1** was maintained constant through the titration. *Solvent residual peak.

The ^{1}H NMR titration spectra of the calix[4]pyrrole **1** with the formamide **5** (Figure S45) showed chemical shift changes on the proton signals of the host upon addition of incremental amounts of the guest. This result was indicative of a fast chemical exchange on the ^{1}H NMR chemical shift

timescale between free and bound receptor. The proton signals of *trans*-**5** appeared sharp and well-defined but they did not display appreciable chemical shift changes respect to the free compound, indicating lack of interaction. The proton signals of *cis*-**5** appeared very broad and upfield shifted with respect to the free *cis*-amide at the initial phase of the titration experiment. This observation indicated that free and bound *cis*-**5** displayed an intermediate chemical exchange on the chemical shift timescale.

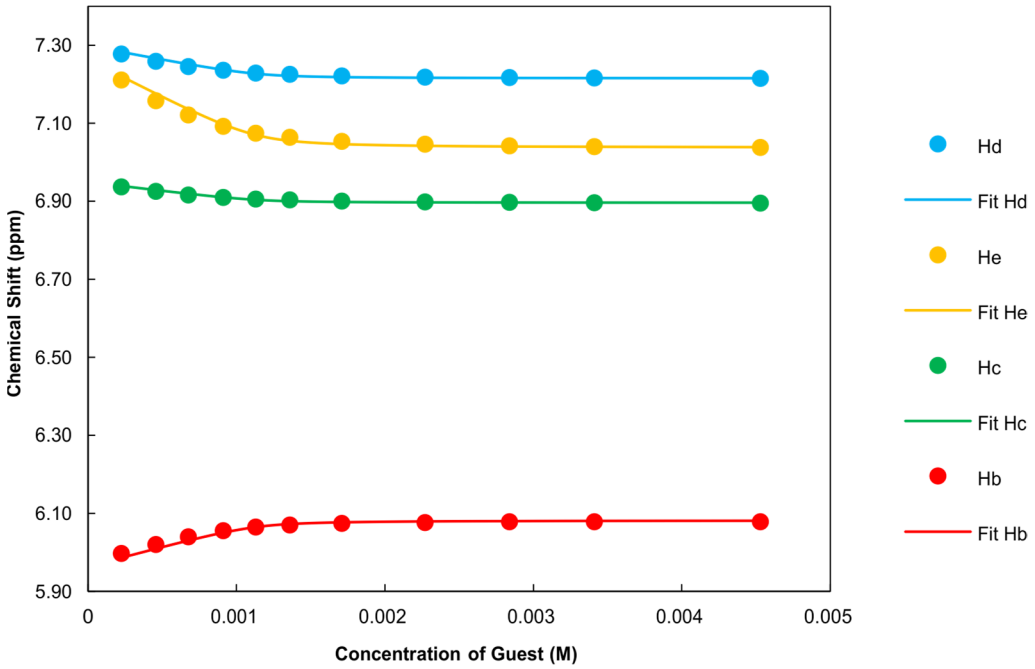

Figure S46. Fit of the ^{1}H NMR titration data (calix[4]pyrrole **1** with **5**) to a theoretical 1:1 binding model.

Table S12. Apparent binding constant returned from the fit of the ^{1}H NMR titration data (calix[4]pyrrole **1** with **5**) to a theoretical 1:1 binding model.

Amide	K_{app} (M^{-1})
5	> 10^4

Table S13. Chemical shifts for the proton signals of bound host **1** (δ_{bound}) obtained from the fit of the ^{1}H NMR titration data (calix[4]pyrrole **1** with **5**) to a theoretical 1:1 binding model and induced chemical shifts ($\Delta\delta = \delta_{bound} - \delta_{free}$).

Signal	δ_{free} (ppm)	δ_{bound} (ppm)	$\Delta\delta$ (ppm)
b	5.97	6.08	+0.11
c	6.95	6.90	-0.05
d	7.30	7.21	-0.09
e	7.28	7.04	-0.24

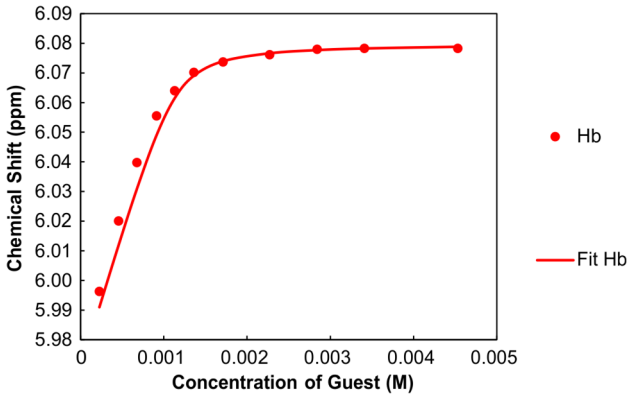

Figure S47. Fit of the ^{1}H NMR titration data (calix[4]pyrrole **1** with **5**) to the theoretical binding model considering the *cis*/*trans* equilibrium and the exclusive formation of the *cis*⊂**1** complex.

Table S14. Binding constant returned from the fit of the ^{1}H NMR titration data (calix[4]pyrrole **1** with **5**) to the theoretical binding model considering the *cis*/t*rans* equilibrium and the exclusive formation of the *cis*⊂**1** complex.

Amide	K_a **(M^{-1})**
cis-**5**	> 10^4

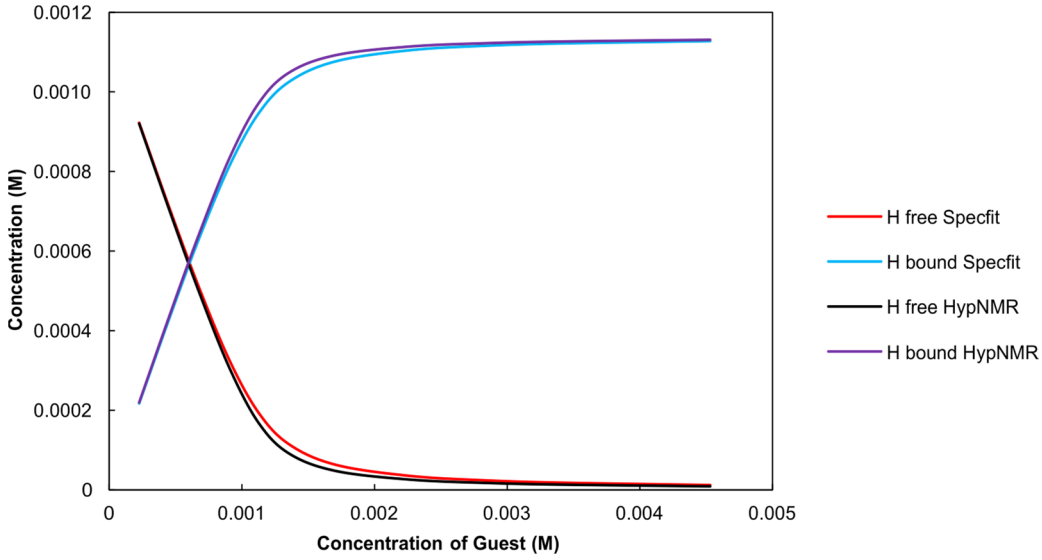

Figure S48. Simulated host (H) speciation profiles using the simple 1:1 binding model (HypNMR) and the theoretical binding model considering the *cis*/*trans* equilibrium and the exclusive formation of the *cis*⊂**1** complex (Specfit).

The speciation profiles obtained by the simple 1:1 binding model and the theoretical binding model considering the *cis*/*trans* equilibrium and the exclusive formation of the *cis*⊂**1** complex were similar. Accordingly, the two binding models returned similar estimates for the binding constant values.

4.5. ^{1}H NMR titration of *N*-methyl-*N*-phenyl-formamide 5 with calix[4]pyrrole 1

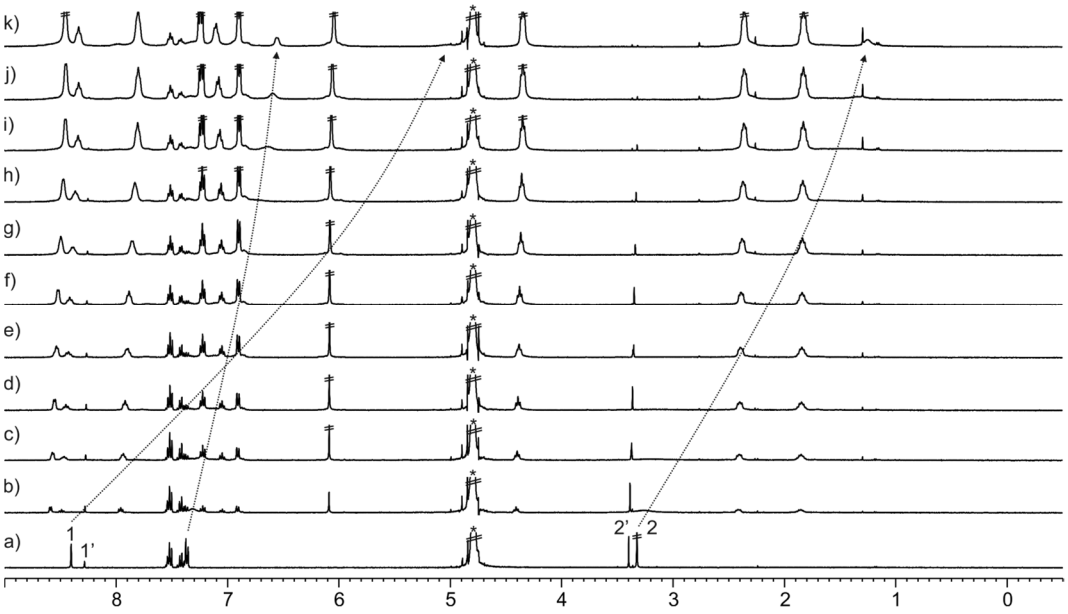

Figure S49. ^{1}H NMR (400 MHz, D_2O, 298 K) titration spectra of *N*-methyl-*N*-phenyl-formamide **5** (2.96 mM) with calix[4]pyrrole **1**: a) **5**; b) **1** + **5** (0.07:1 molar ratio); c) **1** + **5** (0.13:1 molar ratio); d) **1** + **5** (0.2:1 molar ratio); e) **1** + **5** (0.26:1 molar ratio); f) **1** + **5** (0.33:1 molar ratio); g) **1** + **5** (0.5:1 molar ratio); h) **1** + **5** (0.66:1 molar ratio); i) **1** + **5** (1:1 molar ratio); j) **1** + **5** (1.32:1 molar ratio) and k) **1** + **5** (2:1 molar ratio). The concentration of **5** was maintained constant thorough the titration. *Solvent residual peak.

The ^{1}H NMR titration spectra of the formamide **5** with calix[4]pyrrole **1** (Figure S49) showed that the addition of the receptor to a millimolar solution of **5** provoked the broadening and upfield shift of the proton signals of the *cis*-amide **5**. The proton signals of the *trans*-amide **5** (primed numbers) appeared sharp and they did not display appreciable chemical shift changes. However, the *trans*-amide proton signals decreased in intensity due to the intramolecular conformational isomerization of the amide in the bulk solution. The proton signals of the calix[4]pyrrole displayed chemical shift changes with respect to the free receptor in solution. These observations were in line with the results obtained above from the ^{1}H NMR titration experiment of calix[4]pyrrole **1** with formamide **5**.

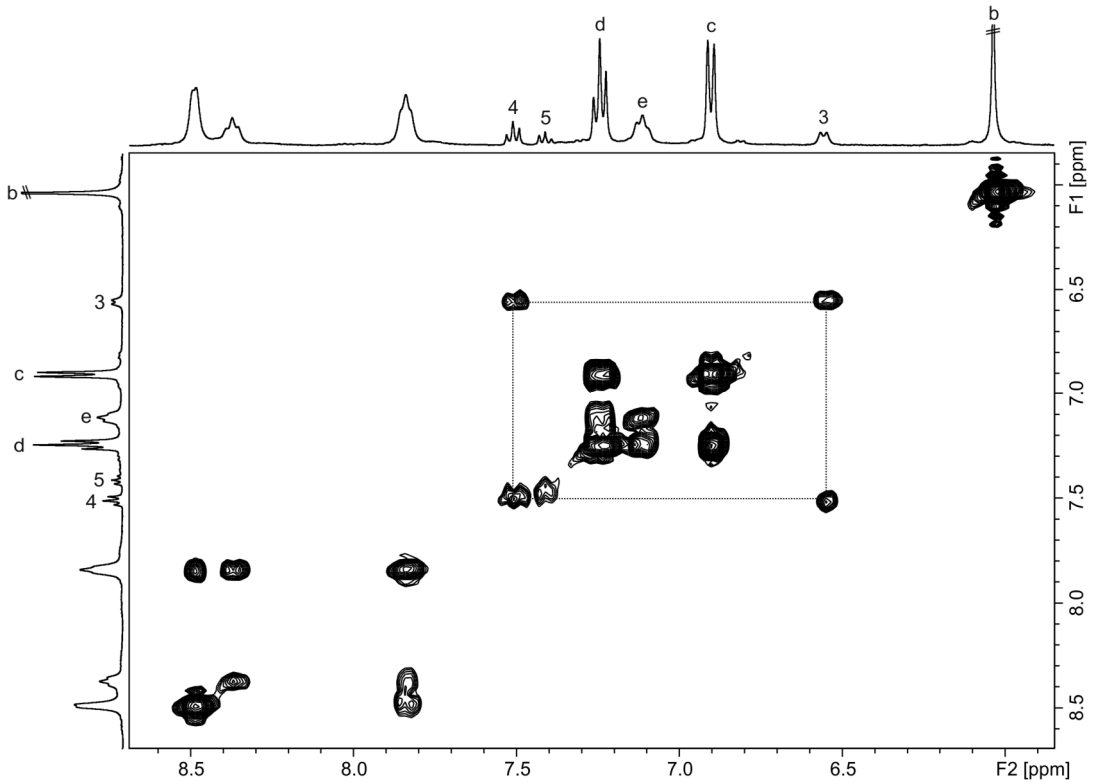

Figure S50. Selected region of the ^{1}H-^{1}H COSY NMR (400 MHz, D_2O, 298 K) spectrum of calix[4]pyrrole **1** and **5** (2:1 molar ratio). COSY cross-peaks between H^3 and H^4 of bound **5** were observed.

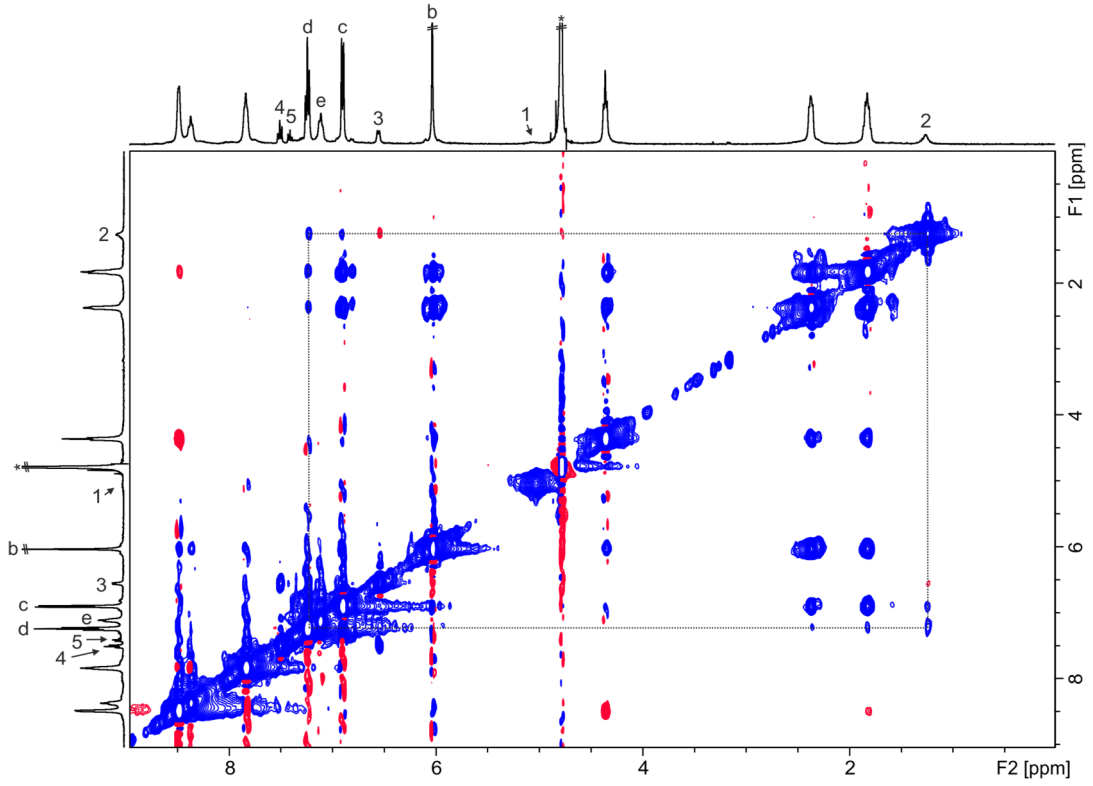

Figure S51. ^{1}H-^{1}H NOESY NMR (400 MHz, D_2O, 298 K, t_{mix} = 0.4 s) spectrum of calix[4]pyrrole **1** and **5** (2:1 molar ratio). NOESY cross-peaks between H^2 of bound **5** and H^c and H^d of calix[4]pyrrole **1** were observed. Also, the NOESY cross-peak between H^2 and H^3 of bound **5** was observed.

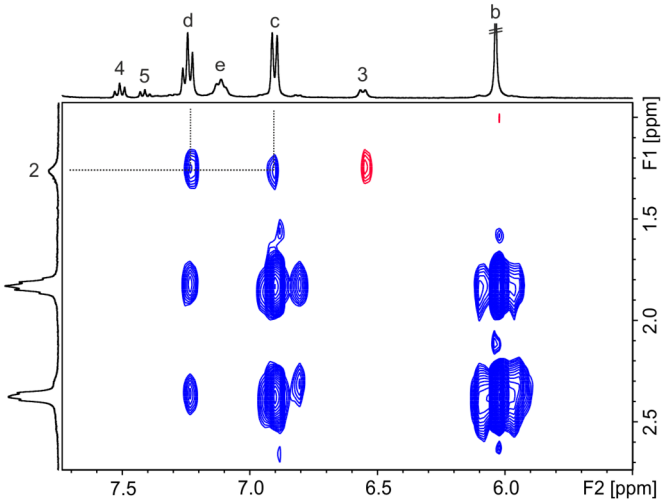

Figure S52. Selected region of the ^{1}H-^{1}H NOESY NMR (400 MHz, D_2O, 298 K, t_{mix} = 0.4 s) spectrum of calix[4]pyrrole **1** and **5** (2:1 molar ratio). NOESY cross-peaks between H^2 of bound **5** and H^c and H^d of calix[4]pyrrole **1** were observed. Also, the NOESY cross-peak between H^2 and H^3 of bound **5** was observed.

Table S15. Experimental (δ_{obs}) and theoretical (δ_t) chemical shifts (ppm) for the proton signals of bound *cis*-**5** with the calix[4]pyrrole **1**. Experimental values were obtained from the mixture of **1** + **5** in a 2:1 molar ratio (Figure S49). The theoretical chemical shifts are in agreement with their observed counterparts.

Signal	δ_{free} (ppm)	δ_{obs} (ppm)	δ_t (ppm)	$\Delta\delta$ (ppm)
1	8.40	5.01	4.70	-3.39
2	3.32	1.25	1.06	-2.07
3	7.36	6.55	5.85	-0.81
4	-	7.43	6.80	-
5	-	7.33	6.69	-

The experimental chemical shift of H^1 in the 2:1 mixture of **1** and **5** was assigned to a broad signal at 5.01 ppm with the help of chemical shift calculations of the *cis*-**5**⊂**1** complex.

4.6. ^{1}H NMR titration of calix[4]pyrrole 1 with *N*-methyl-formamide 6

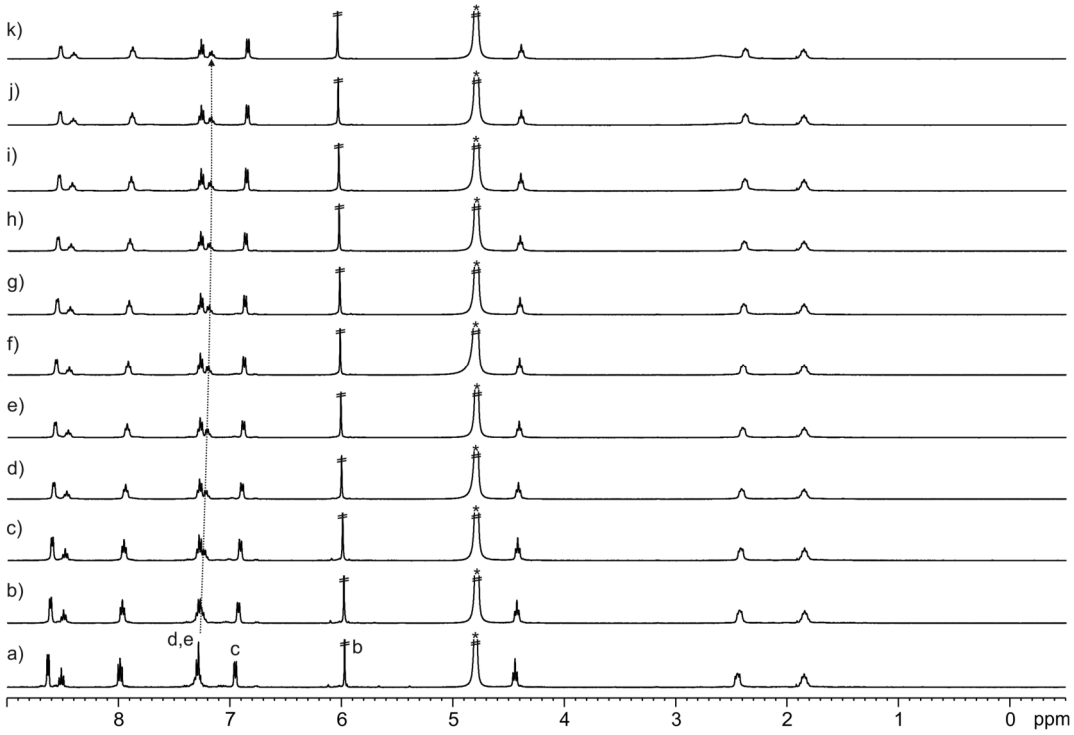

Figure S53. ^{1}H NMR (400 MHz, D_2O, 298 K) titration spectra of calix[4]pyrrole **1** (1.42 mM) with *N*-methyl-formamide **6**: a) **1**; b) **6** + **1** (0.2:1 molar ratio); c) **6** + **1** (0.4:1 molar ratio); d) **6** + **1** (0.6:1 molar ratio); e) **6** + **1** (0.8:1 molar ratio); f) **6** + **1** (1:1 molar ratio); g) **6** + **1** (1.2:1 molar ratio); h) **6** + **1** (1.5:1 molar ratio); i) **6** + **1** (2:1 molar ratio); j) **6** + **1** (3:1 molar ratio) and k) **6** + **1** (5:1 molar ratio). The concentration of **1** was maintained constant through the titration. *Solvent residual peak.

The ^{1}H NMR titration spectra of the calix[4]pyrrole **1** with the formamide **6** (Figure S53) showed chemical shift changes on the proton signals of the host upon addition of incremental amounts of the guest. This result was indicative of a fast chemical exchange on the ^{1}H NMR chemical shift timescale between free and bound receptor. The proton signals of the *trans*- and *cis*-isomers of **6** were not observed at the initial and middle phases and appeared broad at the end of the titration. This observation indicated that free and bound **6** displayed an intermediate chemical exchange on the chemical shift timescale and, most likely, both amide isomers were bound to the calix[4]pyrrole **1**.

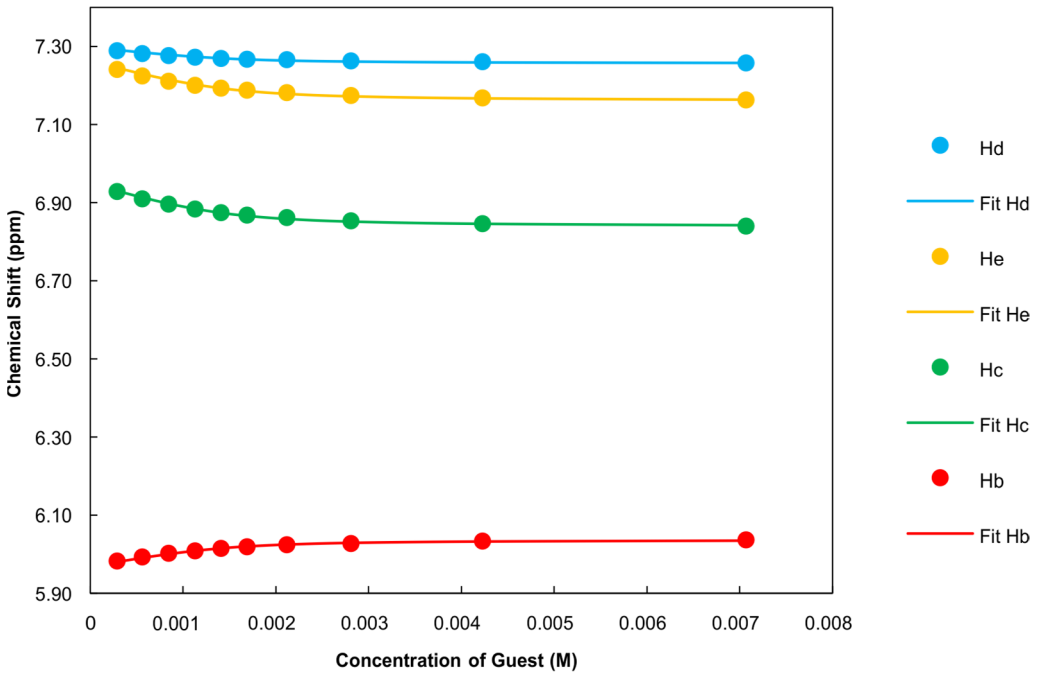

Figure S54. Fit of the ^{1}H NMR titration data (calix[4]pyrrole **1** with **6**) to a theoretical 1:1 binding model.

Table S16. Binding constant returned from the fit of the ^{1}H NMR titration data (calix[4]pyrrole **1** with **6**) to a theoretical 1:1 binding model. The calculated value is the weighted-average of the binding constants of the inclusion complexes of the *cis*- and *trans*-rotamers. Error (standard deviation) is estimated to be lower than 20%.

Amide	K_a (M^{-1})
6	4.4 x 10^3

Table S17. Chemical shifts for the proton signals of bound host **1** (δ_{bound}) obtained from the fit of the ^{1}H NMR titration data (calix[4]pyrrole **1** with **6**) to a theoretical 1:1 binding model and induced chemical shifts ($\Delta\delta = \delta_{bound} - \delta_{free}$).

Signal	δ_{free} (ppm)	δ_{bound} (ppm)	$\Delta\delta$ (ppm)
b	5.97	6.04	+0.07
c	6.95	6.84	-0.11
d	7.30	7.26	-0.04
e	7.28	7.16	-0.12

4.7. ^{1}H NMR titration of *N*-methyl-formamide 6 with calix[4]pyrrole 1

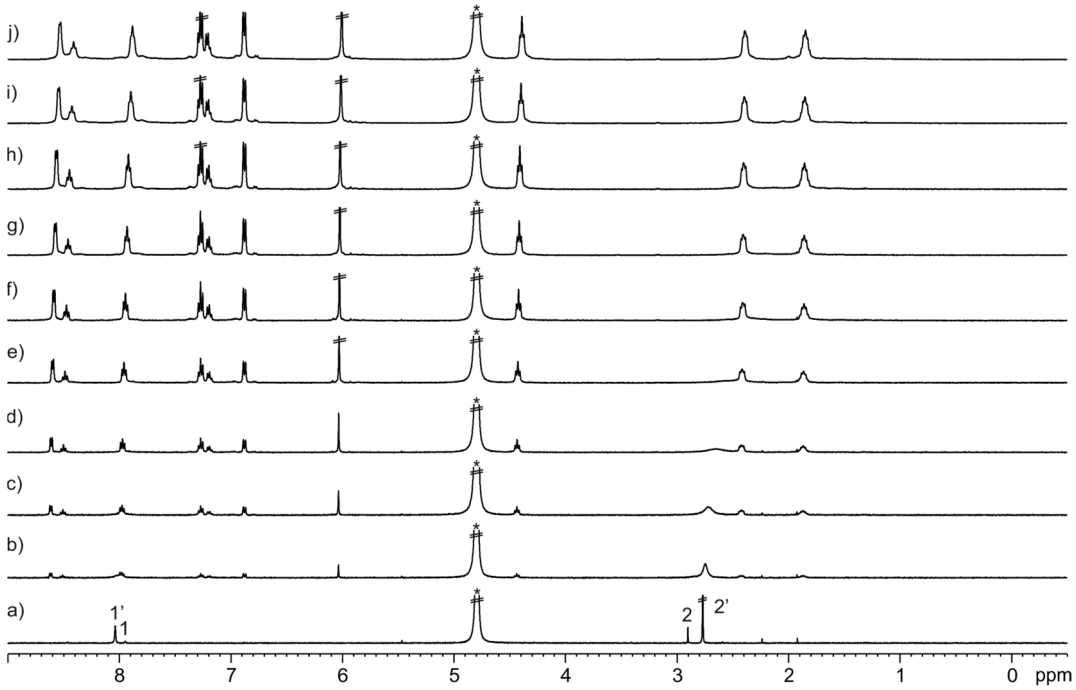

Figure S55. ^{1}H NMR (400 MHz, D_2O, 298 K) titration spectra of *N*-methyl-formamide **6** (1.50 mM) with calix[4]pyrrole **1**: a) **6**; b) **1** + **6** (0.05:1 molar ratio); c) **1** + **6** (0.1:1 molar ratio); d) **1** + **6** (0.2:1 molar ratio); e) **1** + **6** (0.4:1 molar ratio); f) **1** + **6** (0.6:1 molar ratio); g) **1** + **6** (0.8:1 molar ratio); h) **1** + **6** (1:1 molar ratio); i) **1** + **6** (1.5:1 molar ratio) and j) **1** + **6** (2:1 molar ratio). The concentration of **6** was maintained constant through the titration. *Solvent residual peak.

The ^{1}H NMR titration spectra of the formamide **6** with calix[4]pyrrole **1** (Figure S55) showed that the addition of calix[4]pyrrole **1** to a millimolar solution of **6** provoked the broadening and upfield shift of the proton signals of both *trans*- and *cis*-rotamers of **6**. This result indicated that both isomers of **6** interacted with the receptor. The proton signals of the calix[4]pyrrole displayed chemical shift changes with respect to the free receptor in solution. These observations were in line with the results obtained above from the ^{1}H NMR titration experiment of calix[4]pyrrole **1** with formamide **6**.

4.8. ^{1}H NMR titration of calix[4]pyrrole 1 with *N*,*N*-dimethyl-formamide 7

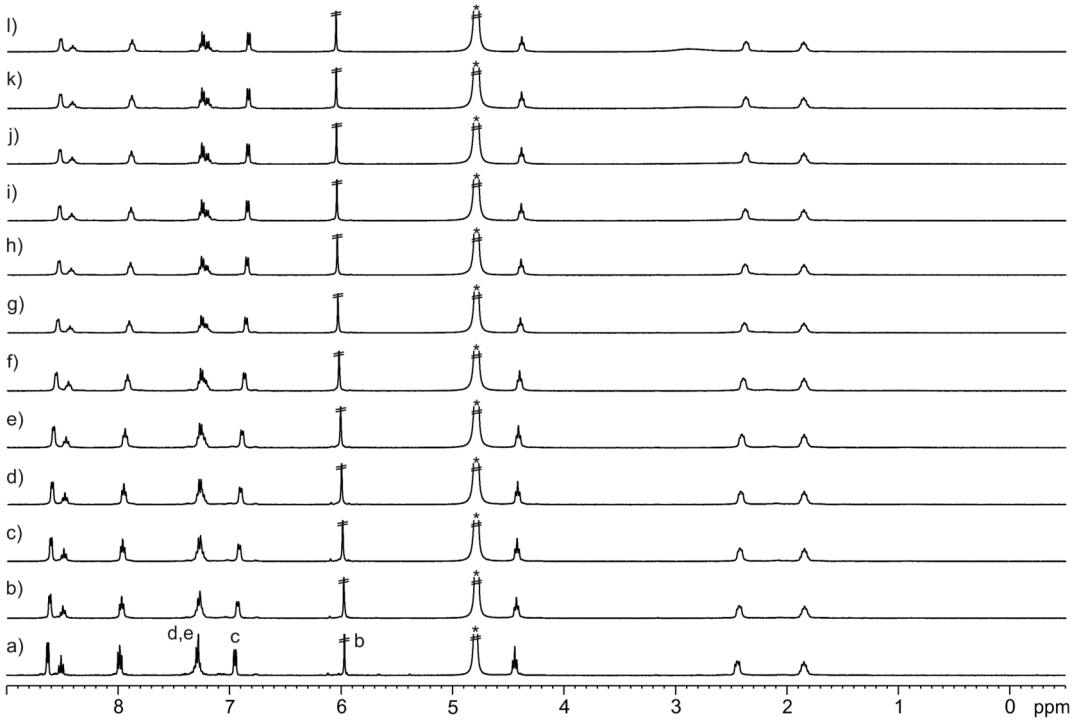

Figure S56. ^{1}H NMR (400 MHz, D_2O, 298 K) titration spectra of calix[4]pyrrole **1** (1.28 mM) with *N,N*-dimethyl-formamide **7**: a) **1**; b) **7** + **1** (0.1:1 molar ratio); c) **7** + **1** (0.2:1 molar ratio); d) **7** + **1** (0.3:1 molar ratio); e) **7** + **1** (0.4:1 molar ratio); f) **7** + **1** (0.6:1 molar ratio); g) **7** + **1** (0.8:1 molar ratio); h) **7** + **1** (1:1 molar ratio); i) **7** + **1** (1.2:1 molar ratio); j) **7** + **1** (1.5:1 molar ratio); k) **7** + **1** (2:1 molar ratio) and l) **7** + **1** (3:1 molar ratio). The concentration of **1** was maintained constant through the titration. *Solvent residual peak.

The ^{1}H NMR titration spectra of the calix[4]pyrrole **1** with formamide **7** (Figure S56) showed chemical shift changes on the proton signals of the host upon addition of incremental amounts of the guest. This result was indicative of a fast chemical exchange on the ^{1}H NMR chemical shift timescale between free and bound receptor. The proton signals of **7** were not observed at the initial and middle phases and appeared broad at the end of the titration. This observation indicated that free and bound **7** displayed an intermediate chemical exchange on the chemical shift timescale.

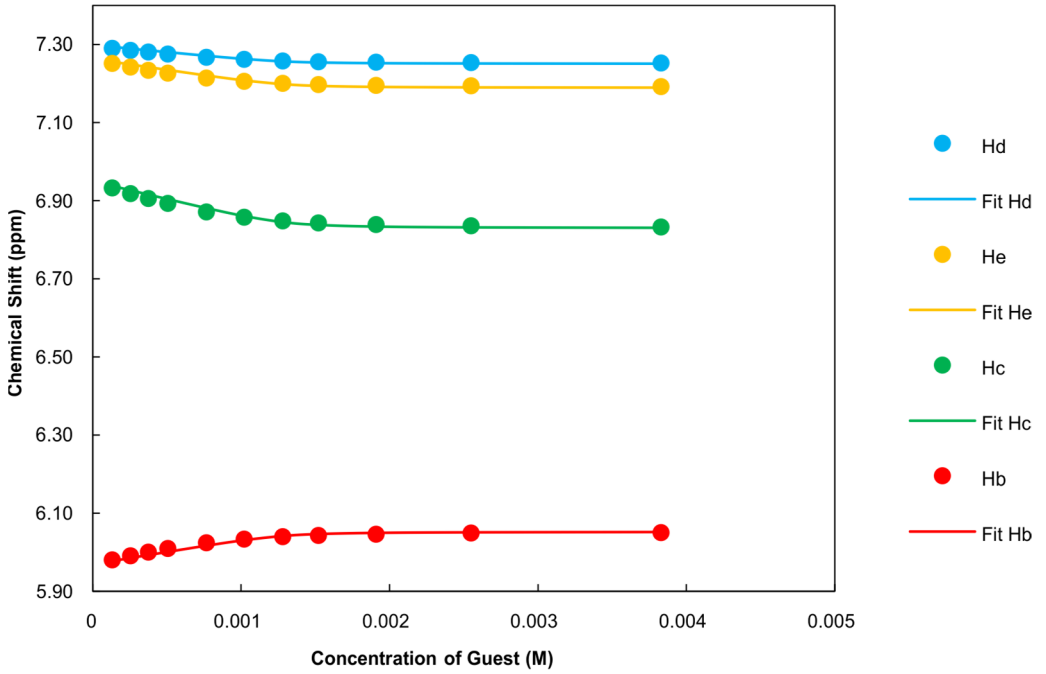

Figure S57. Fit of the ^{1}H NMR titration data (calix[4]pyrrole **1** with **7**) to a theoretical 1:1 binding model.

Table S18. Binding constant returned from the fit of the ^{1}H NMR titration data (calix[4]pyrrole **1** with **7**) to a theoretical 1:1 binding model.

Amide	K_a (M^{-1})
7	> 10^4

Table S19. Chemical shifts for the proton signals of bound host **1** (δ_{bound}) obtained from the fit of the ^{1}H NMR titration data (calix[4]pyrrole **1** with **7**) to a theoretical 1:1 binding model and induced chemical shifts ($\Delta\delta = \delta_{bound} - \delta_{free}$).

Signal	δ_{free} (ppm)	δ_{bound} (ppm)	$\Delta\delta$ (ppm)
b	5.97	6.05	+0.08
c	6.95	6.83	-0.18
d	7.30	7.25	-0.05
e	7.28	7.19	-0.11

4.9. ^{1}H NMR titration of calix[4]pyrrole 1 with acetamide 8

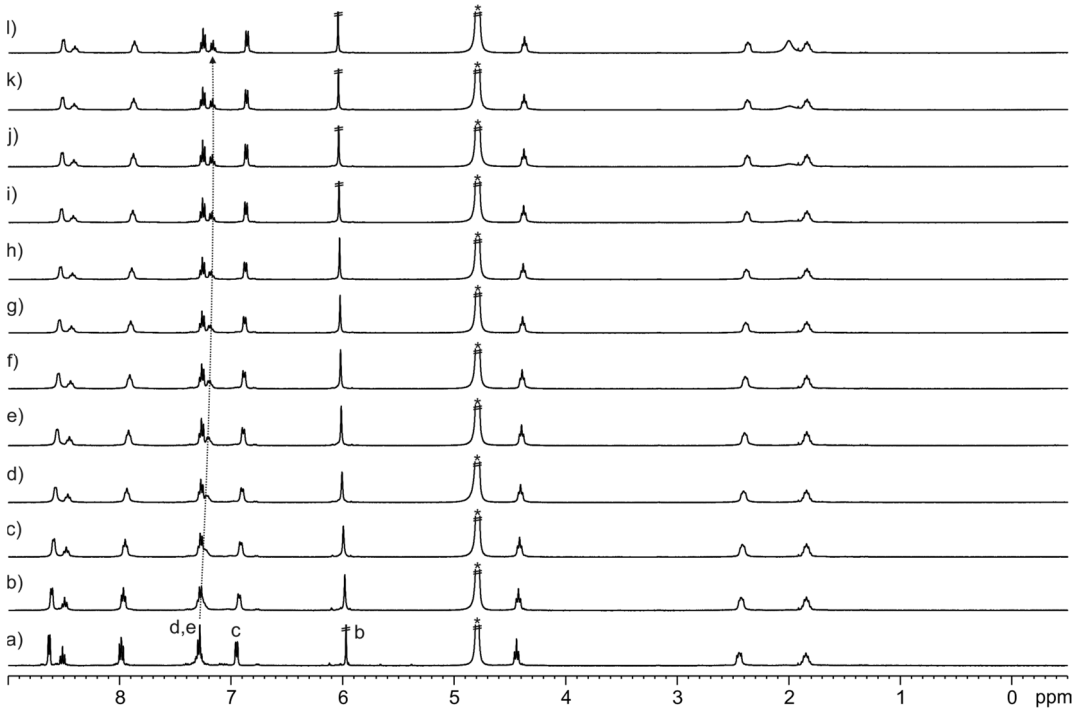

Figure S58. ^{1}H NMR (400 MHz, D_2O, 298 K) titration spectra of calix[4]pyrrole **1** (1.32 mM) with acetamide **8**: a) **1**; b) **8** + **1** (0.2:1 molar ratio); c) **8** + **1** (0.4:1 molar ratio); d) **8** + **1** (0.6:1 molar ratio); e) **8** + **1** (0.8:1 molar ratio); f) **8** + **1** (1:1 molar ratio); g) **8** + **1** (1.2:1 molar ratio); h) **8** + **1** (1.5:1 molar ratio); i) **8** + **1** (2:1 molar ratio); j) **8** + **1** (2.5:1 molar ratio); k) **8** + **1** (3:1 molar ratio) and l) **8** + **1** (5:1 molar ratio). The concentration of **1** was maintained constant through the titration. *Solvent residual peak.

The ^{1}H NMR titration spectra of the calix[4]pyrrole **1** with the acetamide **8** (Figure S58) showed chemical shift changes on the proton signals of the host upon addition of incremental amounts of the guest. This result was indicative of a fast chemical exchange on the ^{1}H NMR chemical shift timescale between free and bound receptor. The proton signal (H^1) of the bound acetamide **8** appeared broad at *ca*. -0.5 ppm. The proton signal of the free acetamide **8** appeared broad at the end of the titration. Most likely, the acetamide **8** displayed an intermediate/slow chemical exchange on the chemical shift timescale.

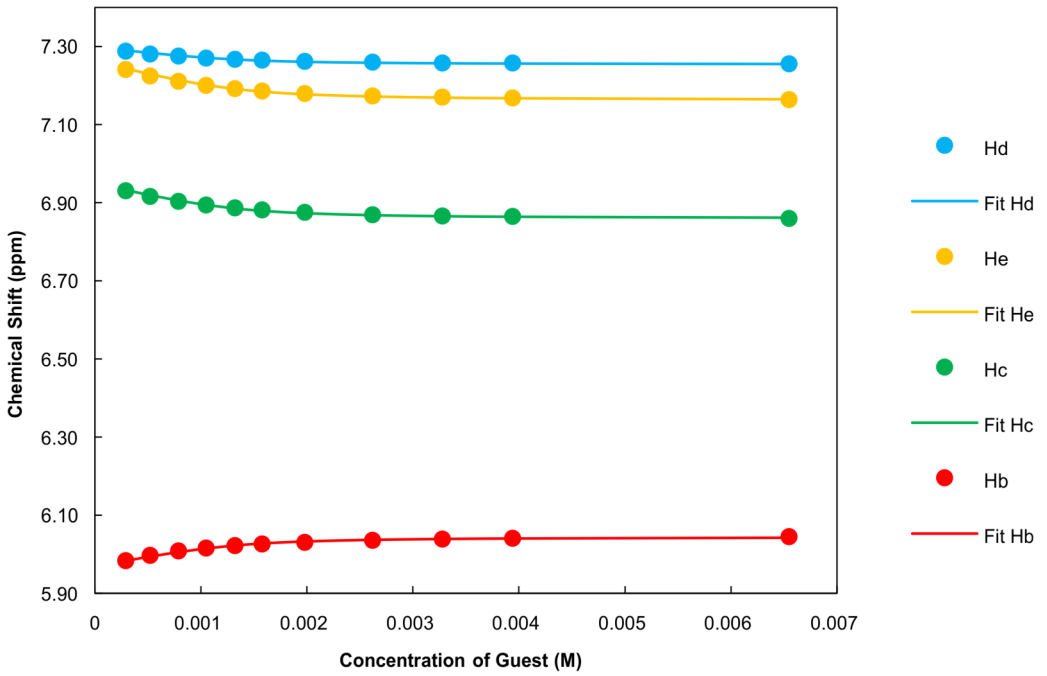

Figure S59. Fit of the ^{1}H NMR titration data (calix[4]pyrrole **1** with **8**) to a theoretical 1:1 binding model.

Table S20. Binding constant returned from the fit of the ^{1}H NMR titration data (calix[4]pyrrole **1** with **8**) to a theoretical 1:1 binding model. Error (standard deviation) is estimated to be lower than 20%.

Amide	K_a (M^{-1})
8	6.8×10^3

Table S21. Chemical shifts for the proton signals of bound host **1** (δ_{bound}) obtained from the fit of the ^{1}H NMR titration data (calix[4]pyrrole **1** with **8**) to a theoretical 1:1 binding model and induced chemical shifts ($\Delta\delta = \delta_{bound} - \delta_{free}$).

Signal	δ_{free} (ppm)	δ_{bound} (ppm)	$\Delta\delta$ (ppm)
b	5.97	6.04	+0.07
c	6.95	6.86	-0.09
d	7.30	7.25	-0.05
e	7.28	7.16	-0.12

4.10. ^{1}H NMR titration of calix[4]pyrrole 1 with *N*-methyl-acetamide 9

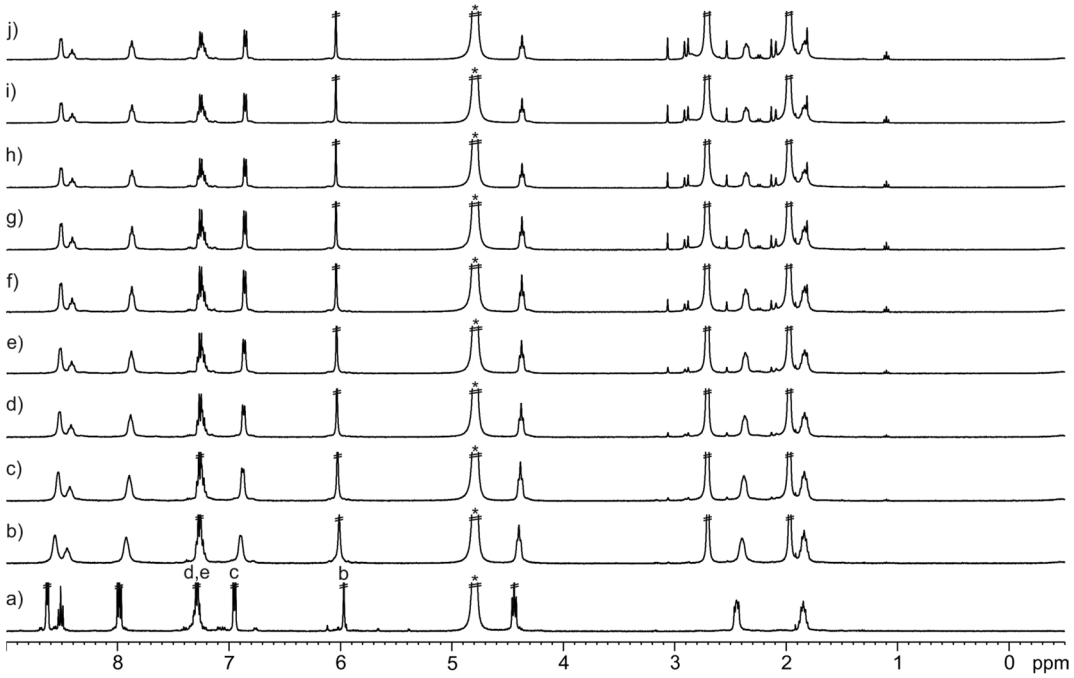

Figure S60. ^{1}H NMR (400 MHz, D_2O, 298 K) titration spectra of calix[4]pyrrole **1** (1.38 mM) with *N*-methyl-acetamide **9**: a) **1**; b) **9** + **1** (5:1 molar ratio); c) **9** + **1** (10:1 molar ratio); d) **9** + **1** (15:1 molar ratio); e) **9** + **1** (20:1 molar ratio); f) **9** + **1** (30:1 molar ratio); g) **9** + **1** (40:1 molar ratio); h) **9** + **1** (50:1 molar ratio); i) **9** + **1** (60:1 molar ratio) and j) **9** + **1** (80:1 molar ratio). The concentration of **1** was maintained constant through the titration. *Solvent residual peak.

The ^{1}H NMR titration spectra of the calix[4]pyrrole **1** with the acetamide **9** (Figure S60) showed small chemical shift changes on the proton signals of the host upon addition of incremental amounts of the guest. This result was indicative of a fast chemical exchange on the ^{1}H NMR chemical shift timescale between free and bound receptor. The proton signal (H^1) of the bound *cis*-acetamide **9** appeared broad at *ca*. -0.5 ppm. Also, the proton signals of the free *trans*-acetamide **9** appeared slightly broad throughout the titration. Most likely, the *cis*-acetamide **9** displayed an intermediate/slow chemical exchange on the chemical shift timescale. The interaction of *trans*-acetamide **9** and calix[4]pyrrole **1** was weak, in line with the results obtained below from the titration experiment with *N*,*N*-dimethyl-acetamide **14**.

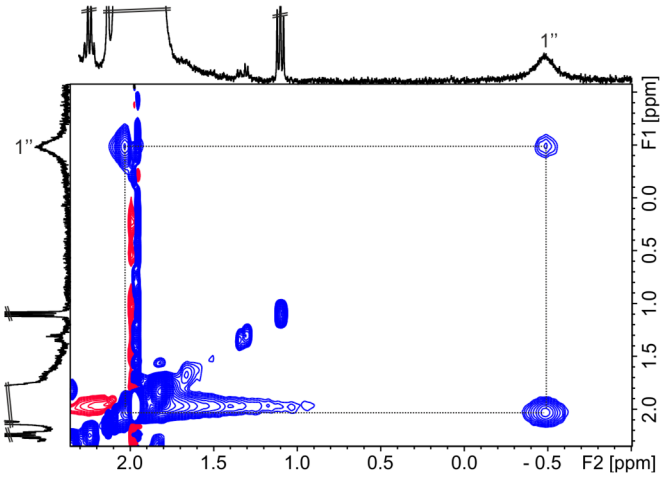

Figure S61. Selected region of the ^{1}H-^{1}H NOESY NMR (400 MHz, D_2O, 298 K, t_{mix} = 0.4 s) spectrum of calix[4]pyrrole **1** and **9** (80:1 molar ratio). Double primed number correspond to proton signal of bound *cis*-**9**.

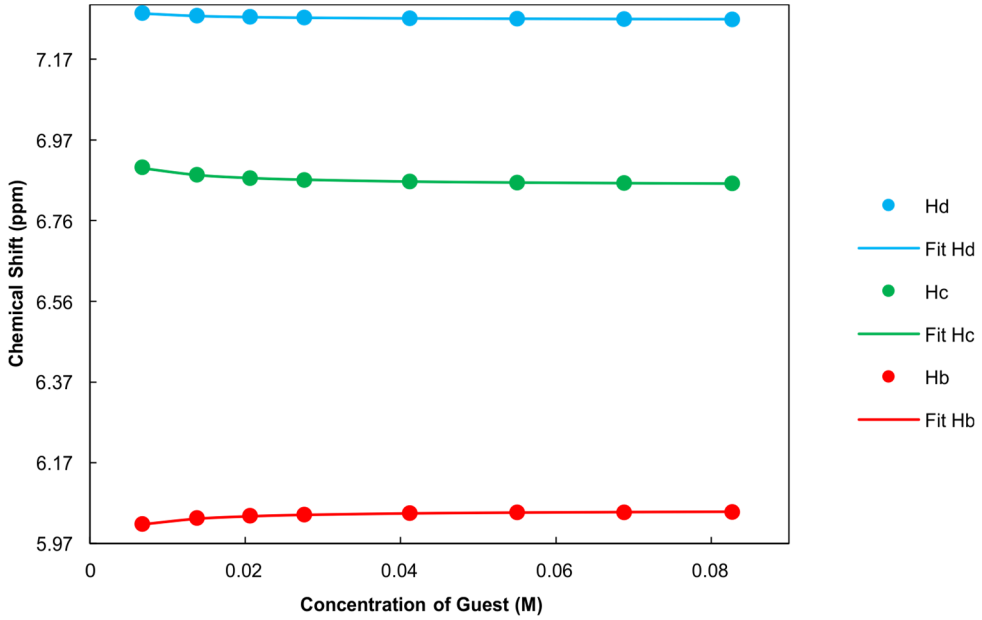

Figure S62. Fit of the ^{1}H NMR titration data (calix[4]pyrrole **1** with **9**) to a theoretical 1:1 binding model.

Table S22. Apparent binding constant returned from the fit of the ^{1}H NMR titration data (calix[4]pyrrole **1** with **9**) to a theoretical 1:1 binding model. Error (standard deviation) is estimated to be lower than 20%.

Amide	K_{app} (M^{-1})
9	2.1 x 10^2

Table S23. Chemical shifts for the proton signals of bound host **1** (δ_{bound}) obtained from the fit of the ^{1}H NMR titration data (calix[4]pyrrole **1** with **9**) to a theoretical 1:1 binding model and induced chemical shifts ($\Delta\delta = \delta_{bound} - \delta_{free}$).

Signal	δ_{free} (ppm)	δ_{bound} (ppm)	$\Delta\delta$ (ppm)
b	5.97	6.05	+0.08
c	6.95	6.85	-0.10
d	7.30	7.26	-0.04

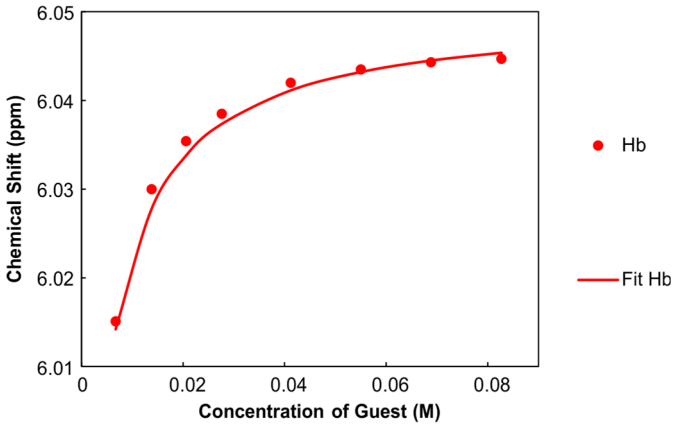

Figure S63. Fit of the ^{1}H NMR titration data (calix[4]pyrrole **1** with **9**) to a theoretical binding model considering the *cis*/*trans* equilibrium and the exclusive formation of the *cis*⊂**1** complex. We considered that the chemical shift value of the *beta*-pyrrole protons in the *cis*-**9**⊂**1** complex was similar to the δ_{bound} value determined from the fit of the titration data to the simple 1:1 binding model.

Table S24. Binding constant returned from the fit of the ^{1}H NMR titration data (calix[4]pyrrole **1** with **9**) to a theoretical binding model considering the *cis*/tr*ans* equilibrium and the exclusive formation of the *cis*⊂**1** complex. Error (standard deviation) is estimated to be lower than 20%.

Amide	K_a (M^{-1})
cis-**9**	1.2 x 10^4

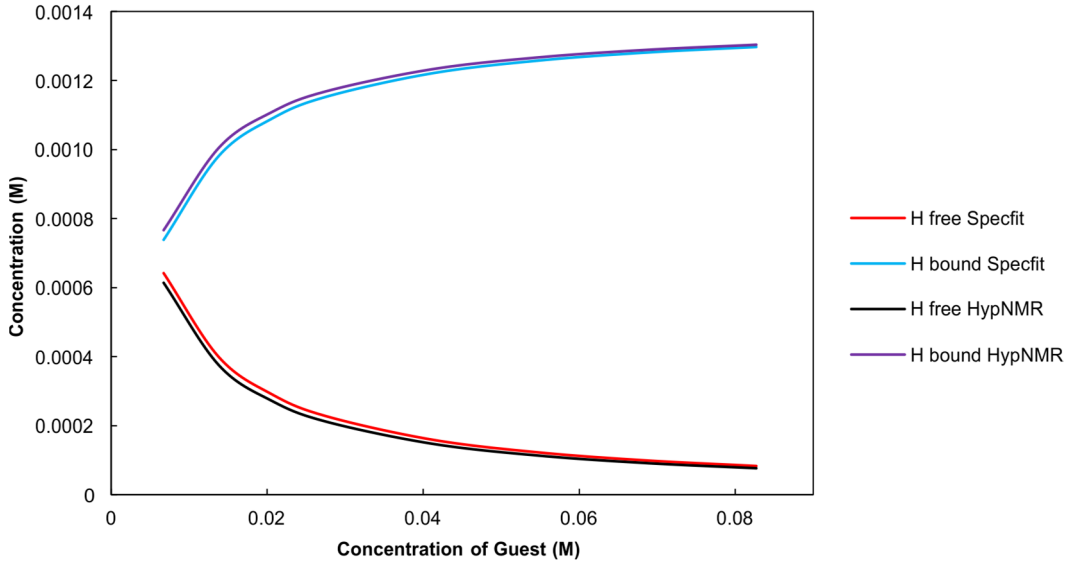

Figure S64. Calculated host (H) speciation profiles using the simple 1:1 binding model (HypNMR) and a theoretical binding model considering the *cis*/*trans* equilibrium and the exclusive formation of the *cis*⊂**1** complex (Specfit).

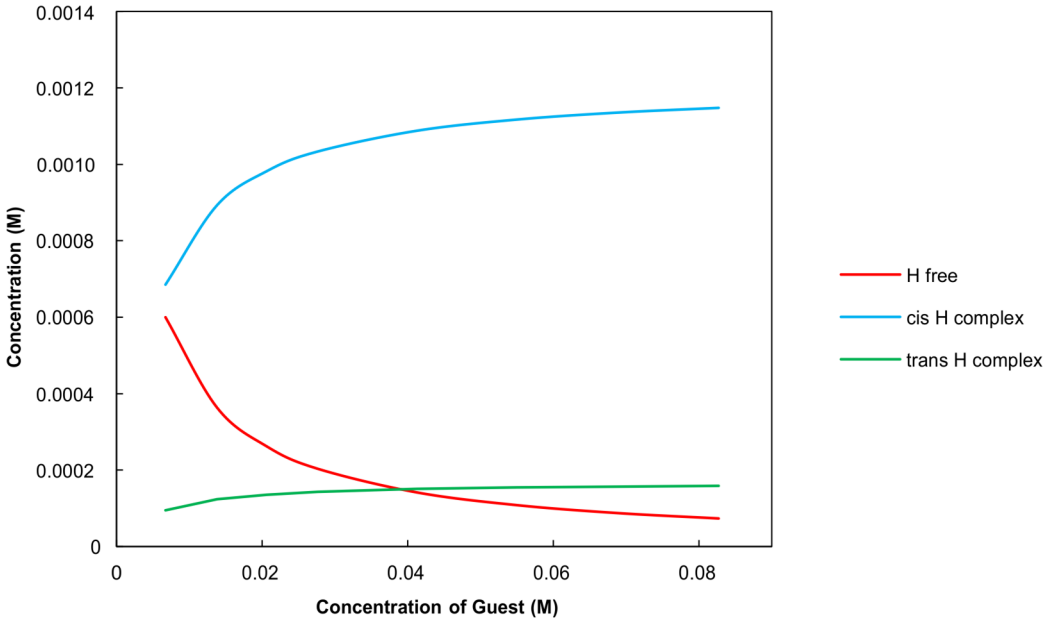

Figure S65. Calculated host (H) speciation profile using the theoretical binding model considering the *cis*/*trans* equilibrium and the formation of the *cis*⊂**1** and *trans*⊂**1** complexes (Specfit): K_a (*cis*⊂**1**) > 10^4 M^{-1}; K_a (*trans*⊂**1**) = 27 M^{-1}; *cis/trans* ratio = 1.6/98.4; [H] = 1.38 x 10^{-3} M.

The value of K_a (*trans*-**9**⊂**1**) was considered similar to the binding constant for the **14**⊂**1** complex (see below). The speciation profile (Figure S65) showed that the *trans*-**9**⊂**1** complex was formed in a reduced extend. For this reason, the *trans*-**9**⊂**1** complex was not included in the fit of the ^{1}H NMR titration data to the theoretical binding model, considering only the *cis*/*trans* equilibrium and the formation of the *cis*-**9**⊂**1** complex.

4.11. ^{1}H NMR titration of calix[4]pyrrole 1 with *N*-phenyl-acetamide 10

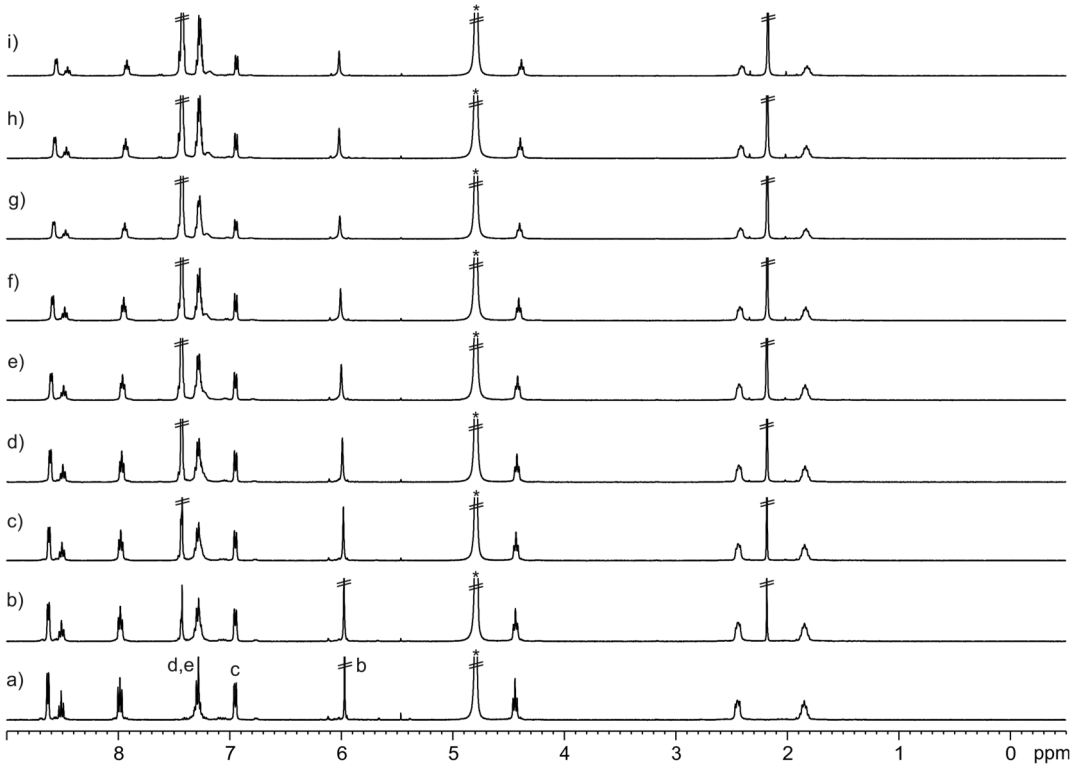

Figure S66. ^{1}H NMR (400 MHz, D_2O, 298 K) titration spectra of calix[4]pyrrole **1** (1.20 mM) with *N*-phenyl-acetamide **10**: a) **1**; b) **10** + **1** (1:1 molar ratio); c) **10** + **1** (2:1 molar ratio); d) **10** + **1** (4:1 molar ratio); e) **10** + **1** (6:1 molar ratio); f) **10** + **1** (8:1 molar ratio); g) **10** + **1** (10:1 molar ratio); h) **10** + **1** (12:1 molar ratio) and i) **10** + **1** (14:1 molar ratio). The concentration of **1** was maintained constant through the titration. *Solvent residual peak.

The ^{1}H NMR titration spectra of the calix[4]pyrrole **1** with acetamide **10** (Figure S66) showed small chemical shift changes on the proton signals of the host upon addition of incremental amounts of the guest. This result was indicative of a fast chemical exchange on the ^{1}H NMR chemical shift timescale between free and bound receptor. The proton signals of *trans*-**10** appeared sharp and well-defined but they did not display appreciable chemical shift changes with respect to the free compound. The proton signals of *cis*-**10** were not observed throughout the titration experiment. Most likely, free and bound *cis*-**10** displayed an intermediate chemical exchange on the chemical shift timescale.

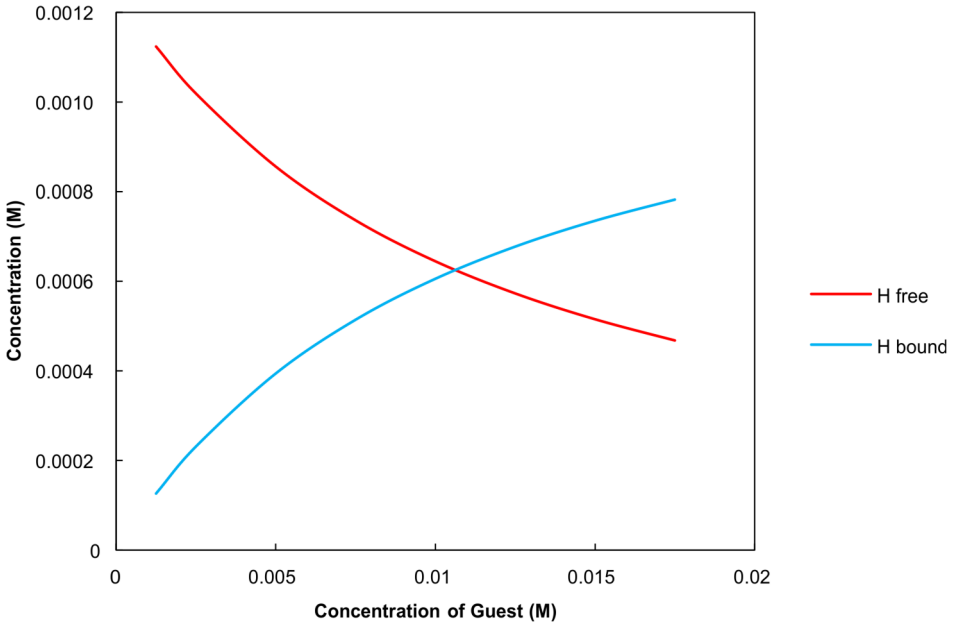

Figure S67. Calculated host (H) speciation profile using a theoretical binding model considering the *cis*/*trans* equilibrium and the exclusive formation of the *cis*⊂**1** complex (Specfit): K_a = 1 x 10^4 M^{-1}; K_{iso} = 1/99; [H] = 1.20 x 10^{-3} M. The simulated speciation profile indicated the formation of the *cis*⊂**1** complex in a considerable extend.

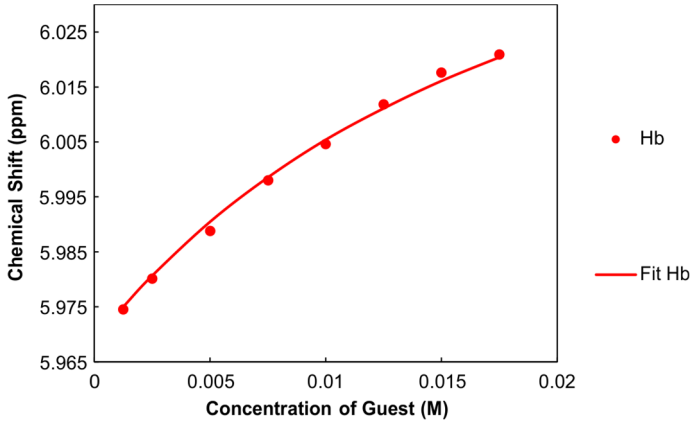

Figure S68. Fit of the ^{1}H NMR titration data (calix[4]pyrrole **1** with **10**) to a theoretical 1:1 binding model.

Table S25. Apparent binding constant returned from the fit of the ^{1}H NMR titration data (calix[4]pyrrole **1** with **10**) to a theoretical 1:1 binding model. Error (standard deviation) is estimated to be lower than 20%.

Amide	K_{app} (M^{-1})
10	51

Table S26. Chemical shifts for the proton signal of host **1** (δ_{free} and δ_{bound}) that were fixed for the fitting of the ^{1}H NMR titration data (calix[4]pyrrole **1** with **10**) to a theoretical 1:1 binding model and induced chemical shifts ($\Delta\delta = \delta_{bound} - \delta_{free}$).

Signal	δ_{free} (ppm)	δ_{bound} (ppm)	$\Delta\delta$ (ppm)
b	5.97	6.08	+0.11

We considered that the chemical shift value of the *beta*-pyrrole protons in the *cis*-**5**⊂**1** complex was a good estimate for δ_{bound} in the *cis*-**10**⊂**1** complex.

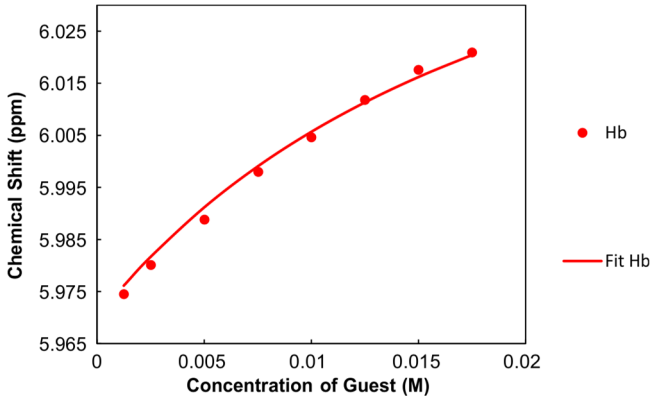

Figure S69. Fit of the ^{1}H NMR titration data (calix[4]pyrrole **1** with **10**) to a theoretical binding model considering the *cis*/*trans* equilibrium and the exclusive formation of the *cis*⊂**1** complex.

Table S27. Binding constant returned from the fit of the ^{1}H NMR titration data (calix[4]pyrrole **1** with **10**) to a theoretical binding model considering the *cis*/*trans* equilibrium and the exclusive formation of the *cis*⊂**1** complex. Error (standard deviation) is estimated to be lower than 20%.

Amide	K_a (M^{-1})
cis-**10**	5.0 x 10^3

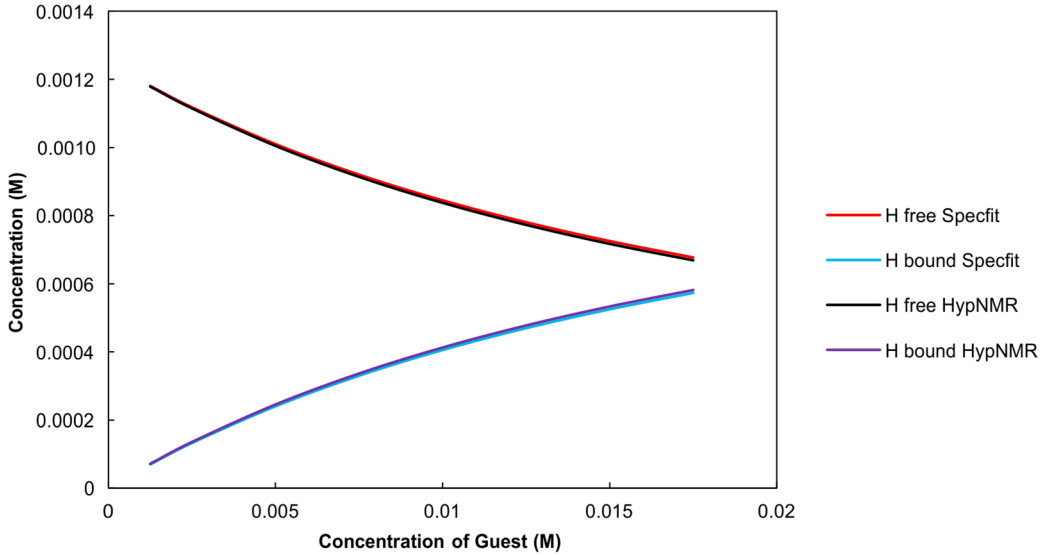

Figure S70. Calculated host (H) speciation profiles using the simple 1:1 binding model (HypNMR) and a theoretical binding model considering the *cis*/*trans* equilibrium and the exclusive formation of the *cis*⊂**1** complex (Specfit).

The speciation profiles obtained by the simple 1:1 binding model and the theoretical binding model considering the *cis*/*trans* equilibrium and the exclusive formation of the *cis*⊂**1** complex are almost identical.

4.12. ^{1}H NMR titration of *N*-phenyl-acetamide 10 with calix[4]pyrrole 1

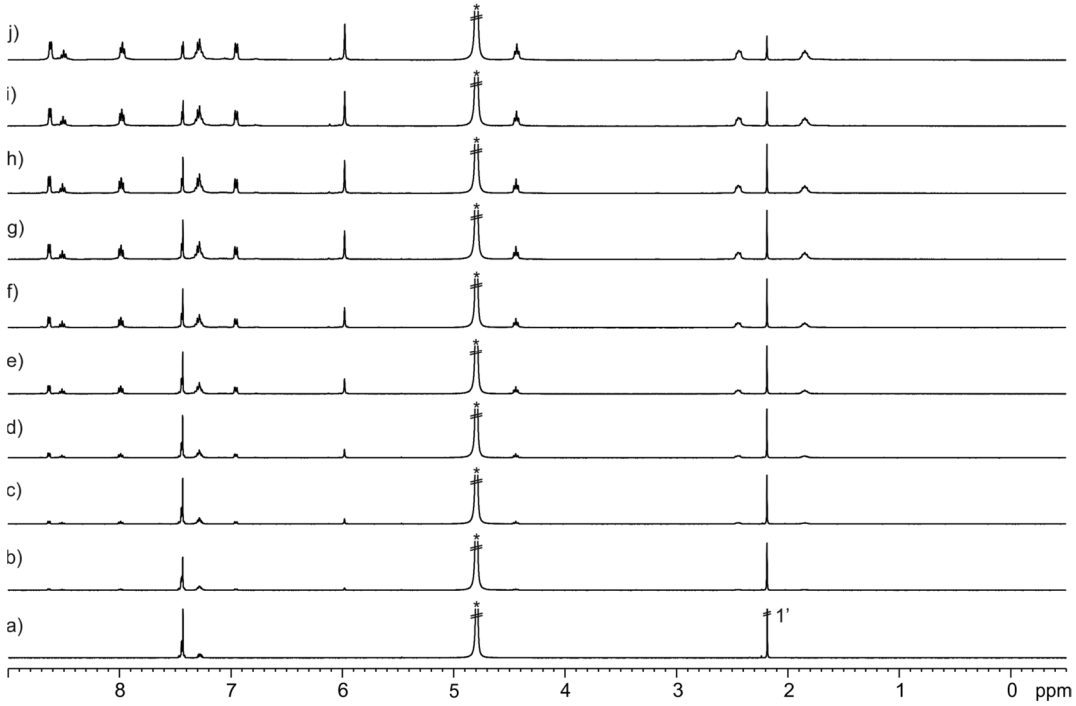

Figure S71. ^{1}H NMR (400 MHz, D_2O, 298 K) titration spectra of *N*-phenyl-acetamide **10** (1.51 mM) with calix[4]pyrrole **1**: a) **10**; b) **1** + **10** (0.05:1 molar ratio); c) **1** + **10** (0.1:1 molar ratio); d) **1** + **10** (0.2:1 molar ratio); e) **1** + **10** (0.4:1 molar ratio); f) **1** + **10** (0.6:1 molar ratio); g) **1** + **10** (0.8:1 molar ratio); h) **1** + **10** (1:1 molar ratio); i) **1** + **10** (1.5:1 molar ratio) and j) **1** + **10** (2:1 molar ratio). The concentration of **10** was maintained constant through the titration. *Solvent residual peak.

The ^{1}H NMR titration spectra of the acetamide **10** with the calix[4]pyrrole **1** (Figure S71) showed that the addition of the receptor to a millimolar solution of **10** provoked the decrease of the intensity of the proton signals of *trans*-**10** (primed numbers) but they did not display appreciable chemical shift changes. This result was indicative of the conformational isomerization of the *trans*- to the *cis*-isomer. The proton signals of the calix[4]pyrrole displayed chemical shift changes with respect to the free receptor in solution. These observations were in line with the results obtained above from the ^{1}H NMR titration experiment of calix[4]pyrrole **1** with acetamide **10**.

4.13. ^{1}H NMR titration of calix[4]pyrrole 1 with *O*-acetotoluidide 11

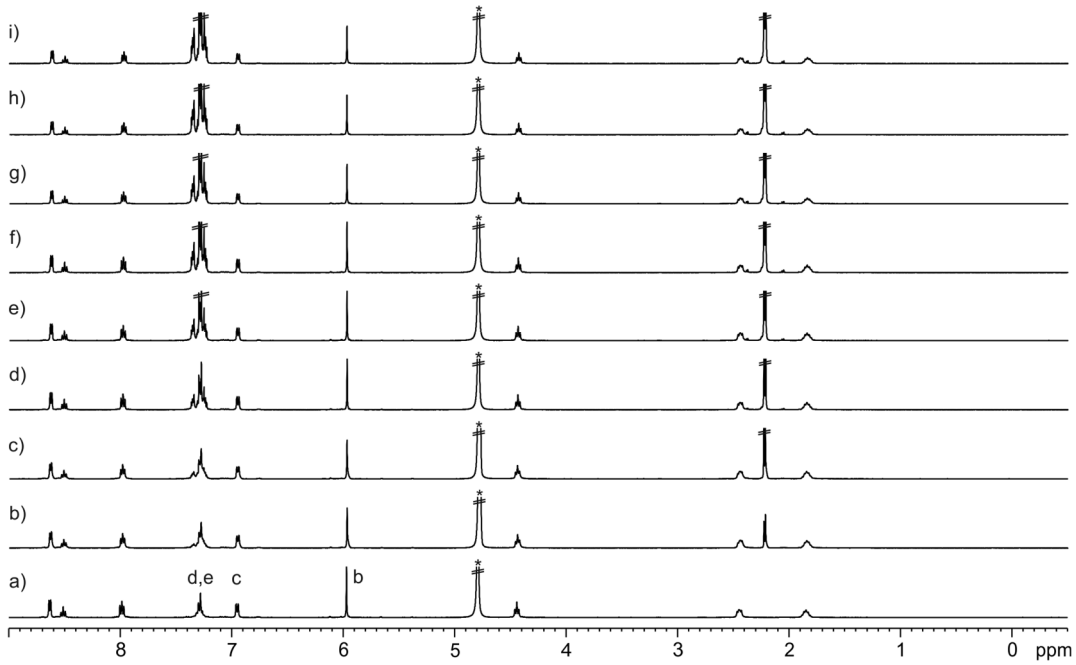

Figure S72. ^{1}H NMR (400 MHz, D_2O, 298 K) titration spectra of calix[4]pyrrole **1** (1.10 mM) with *O*-acetotoluidide **11**: a) **1**; b) **11** + **1** (1:1 molar ratio); c) **11** + **1** (2:1 molar ratio); d) **11** + **1** (4:1 molar ratio); e) **11** + **1** (6:1 molar ratio); f) **11** + **1** (8:1 molar ratio); g) **11** + **1** (10:1 molar ratio); h) **11** + **1** (12:1 molar ratio) and i) **11** + **1** (12.7:1 molar ratio). The concentration of **1** was maintained constant through the titration. *Solvent residual peak.

The ^{1}H NMR titration spectra of the calix[4]pyrrole **1** with acetamide **11** (Figure S72) showed reduced chemical shift changes on the proton signals of the host upon addition of incremental amounts of the guest. This result was indicative of a fast chemical exchange on the ^{1}H NMR chemical shift timescale between free and bound receptor. The proton signals of *trans*-**11** appeared sharp and well-defined but they did not display appreciable chemical shift changes respect to the free compound. The proton signals of *cis*-**11** were not observed throughout the titration experiment. Most likely, free and bound *cis*-**11** displayed an intermediate chemical exchange on the chemical shift timescale.

4.14. ^{1}H NMR titration of *O*-acetotoluidide 11 with calix[4]pyrrole 1

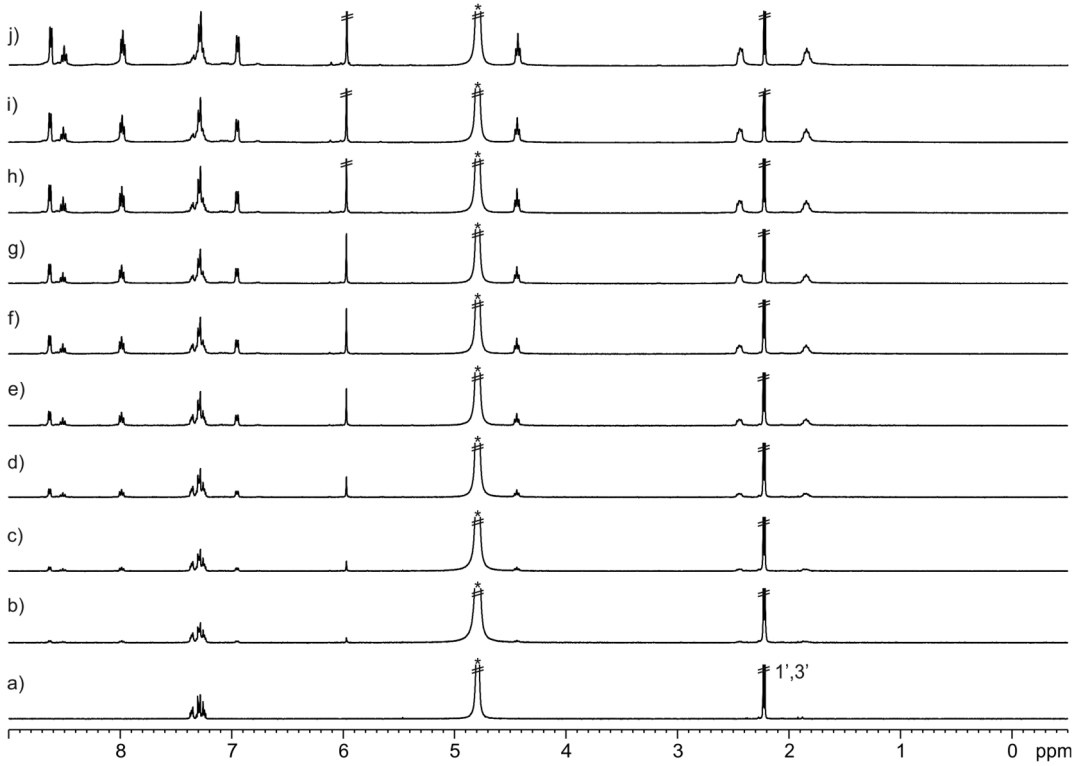

Figure S73. ^{1}H NMR (400 MHz, D_2O, 298 K) titration spectra of *O*-acetotoluidide **11** (1.30 mM) with calix[4]pyrrole **1**: a) **11**; b) **1** + **11** (0.05:1 molar ratio); c) **1** + **11** (0.1:1 molar ratio); d) **1** + **11** (0.2:1 molar ratio); e) **1** + **11** (0.4:1 molar ratio); f) **1** + **11** (0.6:1 molar ratio); g) **1** + **11** (0.8:1 molar ratio); h) **1** + **11** (1:1 molar ratio); i) **1** + **11** (1.5:1 molar ratio) and j) **1** + **11** (2:1 molar ratio). The concentration of **11** was maintained constant through the titration. *Solvent residual peak.

The ^{1}H NMR titration spectra of acetamide **11** with calix[4]pyrrole **1** (Figure S73) showed that the addition of the receptor to a millimolar solution of **11** provoked a reduced decrease of the intensity of the proton signals of *trans*-**11** (primed numbers) but it did not induce appreciable chemical shift changes. This result was indicative of the conformational isomerization of the *trans*-amide to the *cis*-isomer that was selectively bound by **1**. The proton signals of the calix[4]pyrrole **1** also displayed reduced chemical shift changes with respect to the free receptor in solution. These observations were in line with the results obtained above from the ^{1}H NMR titration experiment of calix[4]pyrrole **1** with acetamide **11**.

4.15. ^{1}H NMR titration of calix[4]pyrrole 1 with *N*,*N*-dimethyl-acetamide 14

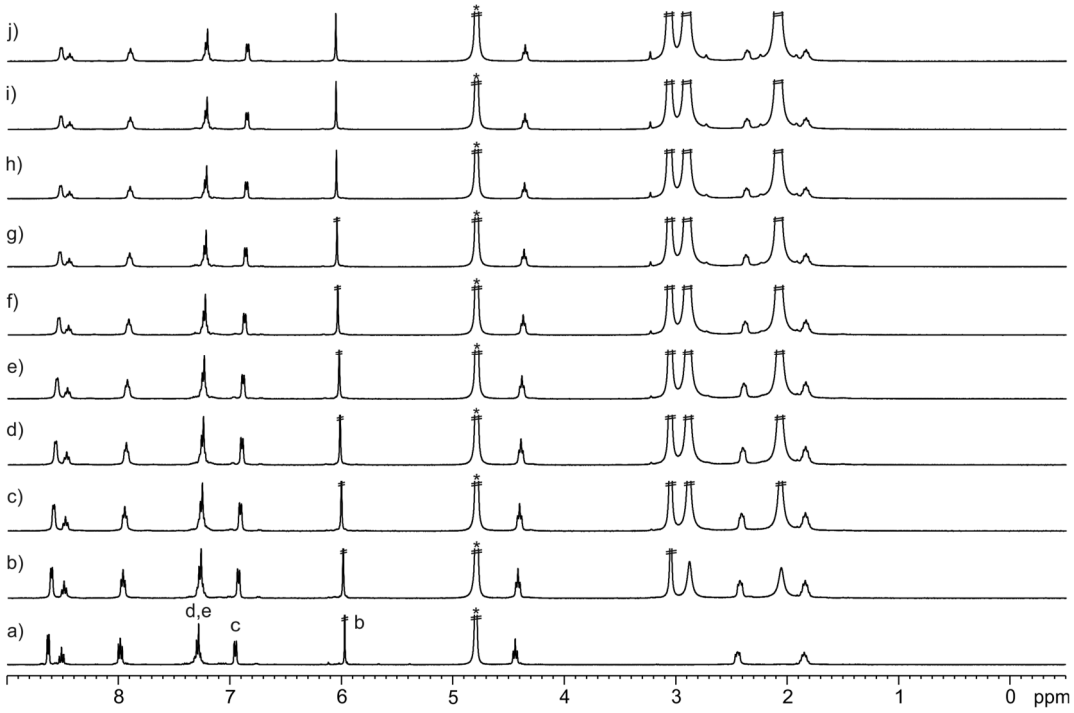

Figure S74. ^{1}H NMR (400 MHz, D_2O, 298 K) titration spectra of calix[4]pyrrole **1** (1.53 mM) with *N,N*-dimethyl-acetamide **14**: a) **1**; b) **14** + **1** (5:1 molar ratio); c) **14** + **1** (10:1 molar ratio); d) **14** + **1** (15:1 molar ratio); e) **14** + **1** (20:1 molar ratio); f) **14** + **1** (30:1 molar ratio); g) **14** + **1** (40:1 molar ratio); h) **14** + **1** (50:1 molar ratio); i) **14** + **1** (60:1 molar ratio) and j) **14** + **1** (70:1 molar ratio). The concentration of **1** was maintained constant through the titration. *Solvent residual peak.

The ^{1}H NMR titration spectra of the calix[4]pyrrole **1** with acetamide **14** (Figure S74) showed small chemical shift changes on the proton signals of the host upon addition of incremental amounts of the guest. This result was indicative of a fast chemical exchange on the ^{1}H NMR chemical shift timescale between free and bound receptor. The proton signals of **14** appeared slightly broadened throughout the titration experiment. This observation indicated that free and bound **14** experienced an intermediate chemical exchange on the chemical shift timescale.

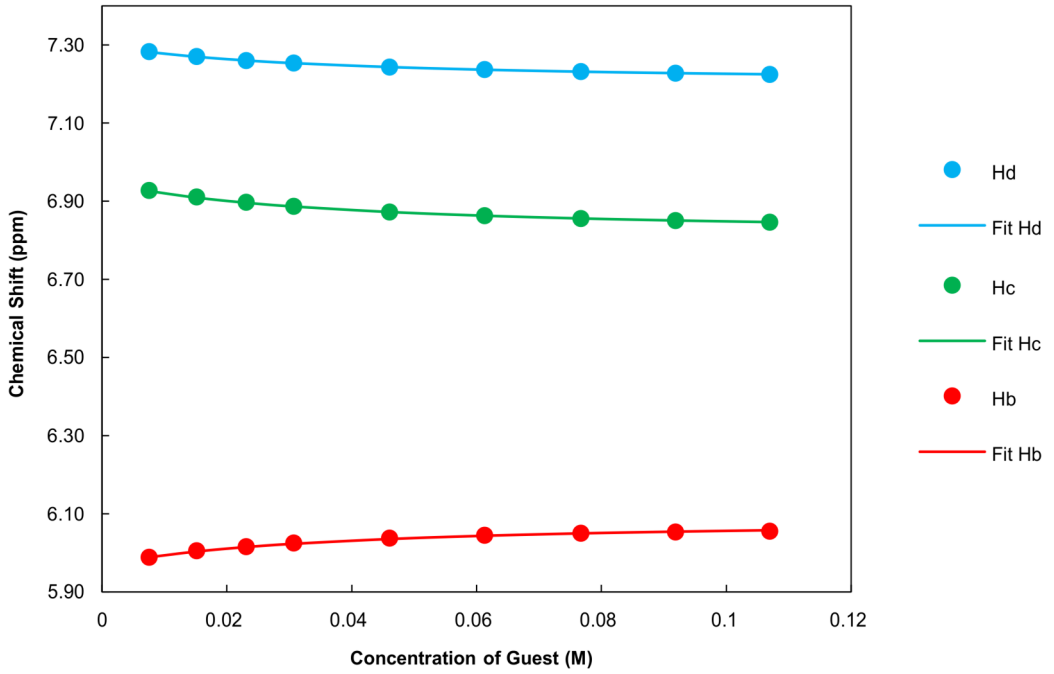

Figure S75. Fit of the ^{1}H NMR titration data (calix[4]pyrrole **1** with **14**) to a theoretical 1:1 binding model.

Table S28. Binding constant returned from the fit of the ^{1}H NMR titration data (calix[4]pyrrole **1** with **14**) to a theoretical 1:1 binding model. Error (standard deviation) is estimated to be lower than 20%.

Amide	K_a (M^{-1})
14	27

Table S29. Chemical shifts for the proton signals of bound host **1** (δ_{bound}) obtained from the fit of the ^{1}H NMR titration data (calix[4]pyrrole **1** with **14**) to a theoretical 1:1 binding model and induced chemical shifts ($\Delta\delta = \delta_{bound} - \delta_{free}$).

Signal	δ_{free} (ppm)	δ_{bound} (ppm)	$\Delta\delta$ (ppm)
b	5.97	6.09	+0.12
c	6.95	6.81	-0.14
d	7.30	7.20	-0.10

5. ITC titration experiments

5.1. ITC titration of calix[4]pyrrole 1 with *N*-methyl-*N*-phenyl-formamide 5

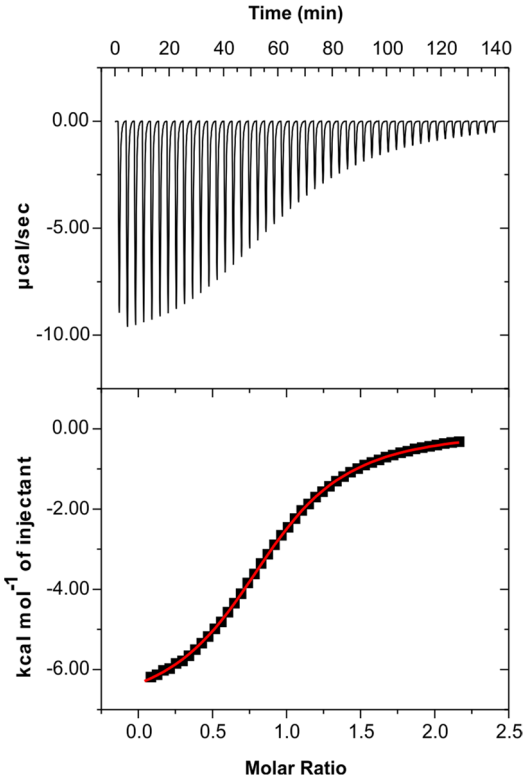

Figure S76. Top) Trace shows raw data for the titration of guest into host: **5**⊂**1**: [**5**] = 10 mM and [**1**] = 0.9 mM. Titration was performed at 298 K. Bottom) Binding isotherm of the calorimetric titration shown on top. The enthalpy of binding for each injection is plotted versus the molar ratio of guest/host in the cell. The continuous line represents the least-squares-fit of the data to the "one set of sites" binding model.

Table S30. Apparent binding constant (K_{app}) and thermodynamic parameters (ΔH, $-T\Delta S$ and ΔG) obtained from the ITC titration experiment at 298 K. Errors in K_{app} and ΔH are reported as standard deviations.

Complex	K_{app} (M^{-1})	ΔH (kcal·mol^{-1})	$-T\Delta S$ (kcal·mol^{-1})	ΔG (kcal·mol^{-1})
5⊂**1**	8.6±0.1 x 10^3	-7.11±0.04	1.75±0.04	-5.36±0.01

The apparent binding constant for the **5**⊂**1** complex was in line with the estimated value returned from the fit of the ^{1}H NMR titration data. The binding of the *N*-methyl-*N*-phenyl tertiary formamide in water was enthalpically driven and entropically opposed.

6. References

[1] Fulmer, G.R.; Miller, A.J.M.; Sherden, N.H.; Gottlieb, H.E.; Nudelman, A.; Stoltz, B.M.; Bercaw, J.E.; Goldberg. K.I. *Organometallics*, **2010**, *29*, 2176–2179.

[2] Díaz-Moscoso, A.; Hernández-Alonso, D.; Escobar, L.; Arroyave, F.A.; Ballester, P. *Org. Lett.* **2017**, *19*, 226-229.

[3] Ahlrichs, R.; Bar, M.; Haser, M.; Horn H.; Kolmel, C. *Chem. Phys. Lett.*, **1989**, *162*, 165-169.

[4] Becke, A.D. *Phys. Rev. A*, **1988**, *38*, 3098-3100.